AD NUMBER

AD278513

LIMITATION CHANGES

TO:

Approved for public release; distribution is unlimited.

FROM:

Distribution authorized to U.S. Gov't. agencies only; Administrative/Operational Use; 15 APR 1962. Other requests shall be referred to Naval Ordnance Lab., Washington, DC.

AUTHORITY

NOL ltr 29 Aug 1974

NOLTR 61-115

AN INVESTIGATION OF THE OPERATING CHARACTERISTICS OF THE SOLID STATE INTENSIFYING SCREENS

15 APRIL 1962

NOL

UNITED STATES NAVAL ORDNANCE LABORATORY, WHITE OAK, MARYLAND

NOLTR 61-115

NOLTR 61-115

AN INVESTIGATION OF THE OPERATING CHARACTERISTICS OF THE SOLID STATE INTENSIFYING SCREENS

Prepared by:

J. A. Holloway

ABSTRACT: This report presents experimental data on the characteristics of the solid state intensifying screens manufactured by the U. S. Radium Corporation under NOrd Contract 18369. Brightness measurements as a function of X-ray intensity from 90 kvp to 10 Mev are given. A comparison of screen characteristics is made relative to a standard fluorescent screen at low X-ray energies and to a NaI crystal at high energies. The increased brightness and contrast of the solid state screen is demonstrated. The equation describing screen brightness in terms of the various screen parameters is derived. Experimental data is given in support of these equations.

PUBLISHED JUNE 1962

U. S. NAVAL ORDNANCE LABORATORY
White Oak, Silver Spring, Maryland

NOLTR 61-115 15 April 1962

AN INVESTIGATION OF THE OPERATING CHARACTERISTICS OF THE SOLID STATE INTENSIFYING SCREENS

The evaluation of two solid state image intensifying screens developed under NOrd Contract 18369 has been carried out under Task RUME 3E 006/212 1/F008 10 004 and RMMP 33 063. This evaluation was to determine the applicability of these screens to the field of industrial radiography. The data is presented in the form of response curves in the voltage range from 90 kvp to 10 Mev. The two screens which have been evaluated represent an initial effort to develop suitable industrial radiographic screens.

The author wishes to acknowledge the general direction and encouragement provided by Mr. George D. Edwards of RUME-322 and Mr. E. E. Katcher of RMMP-43 of the Bureau of Naval Weapons.

W. D. COLEMAN
Captain, U. S. N.
Commander

Zaka I. Slawsky

Z. I. SLAWSKY
By direction

CONTENTS

ILLUSTRATIONS

CONTENTS (Continued)

Figure

INTRODUCTION

1. Fluoroscopy for industrial inspection employs a screen which is limited in sharpness and brightness response. As the usual screens respond linearly to X-ray intensity, the development of a screen with non-linear response greater than one will improve contrast and thus image sensitivity. Solid state intensifying screens offer this characteristic as well as high brightness. A contract was issued to the United States Radium Corporation for the development of two prototype screens with the desired characteristics. 1/ Upon completion of the contract, the screens were evaluated by the Naval Ordnance Laboratory. One screen, no. 251, represents an effort to obtain high brightness with only moderate contrast; the other screen, no. 255, was reported to have a high contrast with lower screen brightness.

2. Emphasis is placed upon evaluating screen brightness at various energies and intensities and determining the decay time. Sensitivity measurements were not attempted due to the small size of the screen (approximately 2 inches by 2 inches) and brightness irregularities across the surface.

3. The brightness of screen no. 251 is given at X-ray intensities of 90, 150, 250 and 2000 kvp and 10 Mev. Due to dielectric breakdown of screen no. 255 no data above 90 kvp was obtained. A comparison of the light output and contrast of screen no. 251 is made relative to a Radelin PFG fluorescent screen*at low X-ray energies and a NaI crystal at higher energies.

4. A theoretical discussion of the operating principles and characteristics of these screens is given first. Then the experimental data are introduced and comparison is made between calculated and experimental results. Finally, attention is drawn to the limitations of the present screens concluding with a discussion of the possible methods of improvement.

THEORETICAL CONSIDERATIONS

5. The term electroluminescent refers to a substance which produces light when excited by an electric field. Pure crystals such as ZnS produce little luminescence. However,

*A zinc sulfide (ZnS) screen manufactured by U. S. Radium.

when a controlled amount of impurity or activator such as Cu_2S is added, the light output is greatly increased. A typical electroluminescent cell is composed of the above constituents suspended in an insulating resin.

6. In order to understand the mechanism of excitation, picture a crystal of activated ZnS in contact with electrodes connected to a voltage source as shown in Figure 1. A potential barrier is established at the interface between the ZnS and the electrode. This barrier is due to electrons which have escaped from donor levels within the ZnS to the electrodes, producing a positive space charge in the ZnS and an equal negative space charge in the electrode. When an electric field is applied, the potential barrier broadens, i.e., the positive space charge increases due to hole transport and entrapment in the activator levels of the cathode region. 2/ Electrons can now penetrate the potential barrier and are accelerated in the surface region by the electric field. Under these conditions they gain enough energy to cause excitation of the activator by impact. For an a-c electroluminescent cell consisting of ZnS grains suspended in an insulating medium it can be assumed that the Cu_2S specks upon the ZnS grains act as the electrodes. 3/ Since these grains are surrounded by resin, contact between the electrodes and the voltage source is not possible. However, when the field is applied, electrons penetrate the barrier producing secondary electrons in the ZnS grains. These are transported through the crystal leaving a positive space charge at the interface and inducing a negative charge within the Cu_2S layer. This lowers the potential and more electrons penetrate the barrier, enlarging the space charge, and so on.

7. Light emission takes place when the free electrons recombine with the holes and the ionized activator centers. The probability that this happens during the excitation process is on the order of 10^{-8} to 10^{-9}. 4/ Thus, the major part of the light output occurs during reversal of the field.

8. The brightness of the electroluminescent (EL) cell therefore depends upon the voltage and frequency across the layer. The fabrication of an image intensifier using an EL layer is possible if a method of modulating the voltage across the layer is devised. Fortunately, photoconductance offers such a method.

9. The impedance of a photoconductive (PC) layer such as CdS, varies with the intensity of the incident radiation. When such a cell is connected with an EL layer across an a-c power supply, the PC layer modulates the voltage drop across the EL layer. An electrical analysis is aided by Figure 2 which shows the PC layer as a capacitor in parallel

with a variable resistor. The EL layer is almost entirely capacitive. It is connected in series with the PC layer across the power supply of voltage, $V = V_o \cos\omega t$.

The voltage fraction across the EL layer is:

$$\frac{V_{2o}}{V_o} = \frac{Z_2}{Z_1+Z_2} \qquad (1)$$

Z_2 = the impedance of the EL layer

Z_1 = the impedance of the PC layer

The emittance B_2 of the EL layer written as a function of the voltage $V_2 = V_{2o} \cos\omega t$ across it is:

$$B_2 = \omega B_2 \propto \exp(-AV_{2o}^{-1/2}) \quad \text{where } \omega = 2\pi f. \ 5/ \qquad (2)$$

$B_2\propto$, and A are constants of the EL layer involved and depend upon layer preparation. V_{2o} is given by equation (1).

10. The impedance or admittance of the layers may be expressed in terms of their capacitance and conductance as follows:

$$\dot{Z}_2 = {}^{1}/\dot{Y}_2 \quad \text{where} \quad \dot{Y}_2 = j\,\omega\,C_2 \qquad (3)$$

$\dot{Y}_2$ = admittance

C_2 = capacitance in farads/m^2

ω = $2\pi f$

The impedance of the PC layer is:

$$\dot{Z}_1 = {}^{1}/\dot{Y}_1 \quad \text{where } \dot{Y}_1 = G_1 + j\,\omega\,C_1 \qquad (4)$$

$\dot{Y}_1$ = admittance of PC layer

G_1 = conductance of PC layer

C_1 = capacitance in farads/m^2

ω = $2\pi f$

Placing (3) and (4) in equation (1) and solving for V_{2o} gives:

$$\left|\frac{V_{20}}{V_0}\right|^2 = \frac{|Z_2^2|}{|Z_1 + Z_2|^2} = \frac{\left|\frac{1}{Y_2}^2\right|}{\left|\frac{1}{Y_1} + \frac{1}{Y_2}\right|^2}$$

$$= \frac{\left|\left(\frac{1}{j\omega C_2}\right)^2\right|}{\left|\frac{1}{G_1 + j\omega C_1} + \frac{1}{j\omega C_2}\right|^2} = \frac{G_1^2 + \omega^2 C_1^2}{G_1^2 + \omega^2(C_1 + C_2)^2}$$

$$V_{20} = V_0\left[\frac{G_1^2 + \omega^2 C_1^2}{G_1^2 + \omega^2(C_1 + C_2)^2}\right]^{\frac{1}{2}} \qquad (5)$$

$$B_2 = \omega B_{2\alpha} \exp\left[-AV_0^{-\frac{1}{2}}\left(\frac{G_1^2 + \omega^2 C_1^2}{G_1^2 + \omega^2(C_1 + C_2)^2}\right)^{-\frac{1}{4}}\right] \qquad (6)$$

11. The conductance of the PC cell (G_1) is a rather complex expression,[6] involving the irradiating intensity and accounting for the absorption of radiation in the layer.

$$G_1 = \frac{\sigma_o}{d_1} + e\mu T\, q\, \frac{I}{d_1}\, f(\alpha d_1) \qquad (7)$$

where

G_1 = conductance of PC cell in ohm^{-1}
σ_o = dark conductivity
e = electronic charge
μ = mobility of the excess charge carriers
T = their lifetime
q = electron equivalent of the radiation
I = radiation intensity in $watts/m^2$
d_1 = thickness of PC layer

The function $f(\alpha,d)$ accounts for layer absorption of the radiation (I). Where the displacement of the charge carriers is small compared to d_1, then:

$$f(\alpha d_1) \approx \frac{d_1^2}{\int_0^{d_1} \frac{1}{\alpha} e^{\alpha x} \, dx}$$

where

α = the linear absorption coefficient of CdS.

As shown in formula (6), the emittance depends upon the relative capacitance of the layers, the applied voltage, the conductance of the PC layer, and the power supply frequency. A plot of the emittance as a function of the irradiating intensity I is shown in Figure 3. This S-shaped curve is characterized by a saturation region at high intensities, a region where the emittance varies with intensity, and a region where brightness is independent of intensity, or low input region.

12. A complete theoretical analysis of the operating characteristics of the screen has been made by Diemer, Klasen, and Santen.[7] A plot of the admittance of a PC cell as a function of frequency is reproduced from this analysis in Figure 4. It can be seen that as the input intensity increases the admittance Y_1 approaches a constant, indicating that the conductance is much greater than the reactance. Thus formula (6) can be simplified for the saturation region and written as

$$B_2 = \omega B_2 \alpha \exp \left[-AV_o^{-1/2} \left(\frac{G_1^2 + \omega^2 C_2^2}{G_1^2} \right)^{1/4} \right] \qquad (8)$$

At intermediate intensities the plot of log B_2 versus X-ray intensity (Figure 3) yields a curve of constant slope γ. Therefore the emittance may be written as:

$$B_2 = K_o I^{\gamma} + K_1 \qquad (9)$$

K_o = proportionality constant

K_1 = displacement constant

γ = contrast amplification

13. At low X-ray intensities the dark conductance (G_{1D}) is a limiting factor and formula (6) takes the form

$$B_2 = \omega B_2 \alpha \exp \left[-\frac{A}{V_o}^{1/2} \left(\frac{G_{1D}^2 + \omega^2 (C_1 + C_2)^2}{G_{1D}^2 + \omega^2 C_1^2} \right)^{1/4} \right] \qquad (10)$$

Further analysis of screen characteristics indicates that contrast amplification and output range (B_2 max - B_2 min) may be increased by making the ratio of the capacitance of the EL layer to that of the PC layer (C_2/C_1) as large as possible. Also the emittance may be expected to increase with both voltage and frequency up to the point of dielectric breakdown of the EL layer.

OPERATING CHARACTERISTICS OF IMAGE INTENSIFIER SCREEN

General

14. The response of an intensifier screen, unlike the standard fluorescent screen, is not a linear function of X-ray intensity. As discussed in the last section, the screen brightness varies with power supply voltage, frequency, X-ray photon energy and intensity. To evaluate the operating characteristics, the screen brightness was measured under these varying conditions. An energy range from 90 kvp to 10 Mev and a frequency range from 100 to 6000 cps was covered. The intensity was varied from approximately 0.1 r/min to 10 r/min.

15. The decay time and sensitivity is another important characteristic. The decay time as a function of frequency was determined for the screens. However, due to their small size (two inches by two inches) radiographic sensitivity was not evaluated.

Experimental Procedure

16. A Model 520 M Photovolt photometer with a 1P21 phototube was used to determine screen brightness. The spectral response of the 1P21 phototube is shown in Figure 5 superimposed upon the response curve of the eye. In order to compensate for the difference in response, a green filter was used in conjunction with the phototube. A one-inch diameter collimator six inches in length was attached to the phototube and screen holder as illustrated in Figure 6.

17. A Macbeth illuminometer was used to find the actual brightness of the Radelin PFG fluorescent screen and the intensifier screen for a given energy and intensity. A plot of this data yields a calibration curve for the photometer readings as a function of the actual screen brightness, Figure 7. There is little difference in the brightness of the yellow Radelin PFG and the blue-green intensifier screens, indicating that the response of the phototube is quite close to that of the eye at these wavelengths.

18. All radiation intensity measurements were made with either a Radacon ratemeter or a Victoreen R-chamber using probes appropriate for the particular energy range.

Experimental Data

19. Brightness measurements were made utilizing the experimental setup shown in Figure 8. These were taken at three power supply frequencies -- 400, 1000 and 6000 cps. The data are plotted for screen no. 251 in Figures 9-13 for X-ray energies of 90 kvp, 150 kvcp, 250 kvcp, 2000 kvp and 10 Mev. Figure 14 is the plot of brightness response for screen no. 255 at 90 kvcp.

20. An evaluation of the screen characteristics over the X-ray energy range is assisted by Table I which gives the maximum screen contrast amplification (γ max) at 400, 1000 and 6000 cps. γ max ranges from 0.63 (2000 kvcp, 400 cps) to 3.1 (250 kvcp, 6000 cps).

TABLE I

γ max for Various Energies - Screen no. 251

Energy	Frequency (cps)		
	400	1000	6000
90 kvp	0.86	1.1	2.1
150 kvp	1.1	1.25	2.6
250 kvcp	1.1	1.5	3.1
2000 kvp	0.63	1.1	1.7
10 Mev		1.0	1.5
	Screen no. 255		
90 kvcp	1.7	2.3	3.0

21. The response of the screen decreases with increasing energy as shown in Figure 15. Maximum brightness occurs near 90 kvp. The response of the Radelin PFG at low energies, and a cylindrical NaI crystal (one-inch diameter by one inch) at the high energies is plotted for comparison.

22. A brightness gain of 25 over the Radelin PFG screen is possible at low energies. The intensifier screen also shows a gain of 12 and 7 over the NaI crystal at 2000 kvp and 10 Mev, respectively.

23. Since the brightness curve is S-shaped the brightness and intensity range may be determined by limiting operation to those regions on the curve where the contrast amplification is 1.0 or greater. Table II is constructed using this criterion. Here the radiation intensity range is given with an associated brightness range for an operating frequency of 1000 cps.

24. The intensity range falls between 0.1 r/min and 19 r/min, while the brightness ranges from 0.0075 ml to 2.0 ml for the no. 251 screen. The greatest intensity and brightness range occurs at 250 kvcp. Screen no. 255 has a greater brightness and intensity range than screen no. 251 at 90 kvp although over-all brightness is much lower.

25. The variation in brightness as a function of frequency is plotted in Figures 16-20 for low, intermediate, and high X-ray intensity levels for both screens. In general, the brightness increases almost linearly with frequency at high intensity levels. At 2000 kvp the curve for 8.8 r/min peaks at 1500 cps, however it can be seen from Figure 12 that at this intensity the screen is still operating in the intermediate region. As the intensity level decreases, brightness increases to a peak value, then decreases again. The lower the intensity the lower the frequency at which this peak occurs. Figure 21 shows a plot of operating frequency as a function of the X-ray intensity for both screens at 90 kvp and at 2000 kvp for screen no. 251. The linear relationship between frequency and X-ray intensity is evident.

TABLE II

Intensity and Brightness Ranges for Various Energies
300 volts - 1000 cps

Energy	Intensity Range (r/min)	Intensity Ratio	Brightness Range (ml)	Brightness Ratio
		Screen no. 251		
90 kvp	0.1-1.0	10	0.04-1.6	40
150 kvcp	0.085-1.5	18	0.016-2.3	144
250 kvcp	0.18-4.0	28	0.01-3.0	300
2000 kvp	1.0-19	19	0.0075-0.7	93
10 Mev	2.0->15	>7.5	0.025->0.3	>12
		Screen no. 255		
90 kvcp	0.4-5.0	12	0.0045-0.65	144

Screen Decay

26. Decay time measurements were made for screen no. 251 at 90 kvp and 2000 kvp. These curves are shown in Figures 22 and 23 while Figure 24 is the curve for screen no. 255 at 90 kvcp. The decay time is defined here as the time required for the screen brightness to reach two percent of its initial value. The decay time is seen to decrease with increasing frequency. At 6 kc this is $\sim$ 30 sec for screen no. 251, compared to $\sim$ 5 sec for screen no. 255. It is also apparent that the decay is energy dependent. Figure 23 shows the decay time to be much greater at 2000 kvp than at 90 kvp for screen no. 251.

27. A Feather analysis was made by constructing a tangent to the decay curve where it becomes a straight line. This is shown in Figure 22 for screen no. 251 at 90 kvp. The brightness difference between this tangent and the original curve is plotted and another tangent constructed. The determination of the slope of these tangents allows an equation to be written for the original curve of the form:

$$B_2 = K_1 e^{-\lambda_1 t} + K_2 e^{-\lambda_2 t} + \ldots$$

This analysis was carried out for frequencies of 400, 1000 and 6000 cps at 90 kvp and 2000 kvp. Table III gives the values of K and λ obtained and the resulting brightness decay equation.

Initial Brightness Buildup

28. The long decay time illustrates one of the characteristics of the screens. Another associated characteristic is the initial buildup of emittance at low operating frequencies. Figure 25 illustrates this for screen no. 251 at 90 kvp. Curve (2) shows the emittance after ten seconds. Curve (1) is a plot of brightness after a steady state condition has been reached. The ten-second curve is S-shaped but the emittance is lower than the steady state curve. As the frequency increases this effect decreases.

Latent Image Formation

29. It was observed that a latent image could be "burned" into the screen, i.e., the image would return after voltage removal and then reapplication along with X-radiation. The time required for the screen to "repair" itself between voltage removal and reapplication was not determined, but it is excessive. The image may be removed by radiating the entire screen with X-rays of high intensity.

TABLE III

Decay Curve Equation Data

Frequency at 90 kvp	λ_1	λ_2	λ_3	K_1	K_2	K_3	Equation
400	--	0.154	0.0162	--	0.170	0.12	$B_2 = 0.170\ e^{-0.154t} + 0.12\ e^{-0.0162t}$
1000	--	0.193	0.0262	--	0.197	0.093	$B_2 = 0.197\ e^{-0.193t} + 0.093\ e^{-0.0262t}$
6000	0.438	0.123	0.012	0.24	0.045	0.0066	$B_2 = 0.24\ e^{-0.438t} + 0.045\ e^{-0.123t} + 0.0066\ e^{-0.012t}$
Frequency at 2000 kvp							
400	--	0.0756	0.00855	--	.034	.096	$B_2 = .034\ e^{-0.0756t} + 0.096\ e^{-0.00855t}$
1000	--	0.0279	0.014	--	.052	.078	$B_2 = .052\ e^{-0.0279t} + .078\ e^{-0.014t}$
6000	--	0.126	0.0176	--	.086	.076	$B_2 = 0.086\ e^{-0.126t} + 0.076\ e^{-0.0176t}$

NOLTR 61-115

Discussion of Results

30. One of the unknown quantities of equation (6), the value of (A), can be obtained from the curves of Figures 16 and 17. With (A) known, some idea of the conductance can be ascertained.

31. Equation (8) for the emittance at high X-ray intensities is based upon the assumption that the conductance of the PC layer is greater than the reactance. The equation if written as

$$B_2 = \omega B_{2\alpha} \exp\left[\frac{-A}{V_o} 1/2 \left(1 + \frac{\omega^2 C_2^2}{G_1^2}\right)^{1/4}\right]$$

reduces to

$$B_2 = \omega B_{2\alpha} \exp \frac{-A}{V_o} 1/2$$

if

$$G_1^2 > \omega^2 C_2^2 \quad \text{and} \quad \left(1 + \frac{\omega^2 C_2^2}{G_1^2}\right)^{1/4} \rightarrow 1 \text{ at saturation.}$$

32. A plot of B_2 vs $\frac{1}{V_o} 1/2$ from Figures 16 and 17 is shown in Figure 26. The points plotted were taken for screen no. 251 operating at 6000 cps and at a saturating X-ray intensity level. The line intersects the ordinate giving the value of

$$\omega B_{2\alpha} = 1.3 \times 10^4 \text{ lumen/m}^2\text{/cycle.}$$

The equation of this line is of the form:

$$P = P_o e^{-\mu x} \tag{12}$$

where

$P = B_2$

$P_o = \omega B_{2\alpha}$

$\mu = A$

$x = \frac{1}{V_o} 1/2$

At the point on the curve corresponding to 200 volts,

$B_2 = 28$ lumen/m^2, $\omega B_{2\alpha} = 1.3 \times 10^4$ lumen/m^2/cycle and

$\frac{1}{V_o} 1/2 = 0.059.$

Substitution of these values in equation (12) gives $\mu = A = 103$.

33. The dark conductance of the PC layer (G_{1D}) can be obtained by substitution of the values for A, B_2, and $\omega B_{2\alpha}$ into equation (10). B_2, as shown in Figure 9, is approaching 0.01 ml (0.1 lumen/m^2) at 200 volts and at low X-ray intensities. The values for the capacitance of the PC and EL layers are 9.8×10^{-10} farad and 3.64×10^{-9} farad respectively, see Appendix A. Substitution of these values into equation (10) yield a value for $G_{1D} = 2.9 \times 10^{-5}/\Omega$ (Appendix B).

34. A check on the value of G_{1D} was obtained by measuring the current and phase angle without irradiation but with 200 volts, 6000 cps on the screen. The screen current was 12 ma while oscilloscope measurement gave a phase angle of 90°. The equivalent electrical circuit of Figure 2 shows the following relationships between voltages and current in the PC and EL layers.

$$\dot{V} = \dot{V}_1 + \dot{V}_2 \qquad \text{where } \dot{V}_1 = \dot{I}_1\dot{Z}_{c_1} = \dot{I}_3 R = \frac{\dot{I}_3}{G_1}$$

$$\dot{V}_2 = \dot{I}_2\dot{Z}_{c_2}$$

and

$$\dot{I} = \dot{I}_1 = \dot{I}_2 + \dot{I}_3$$

A graphical solution is given in Figure 27a. The dark conductance is $G_{1D} = \frac{I_3}{V_1} = 6.9 \times 10^{-5}/\Omega$. This is the correct order of magnitude when compared to the calculated value of $2.9 \times 10^{-5}/\Omega$.

35. The conductance during irradiation was obtained under the same operating conditions but with 14.5 r/min on the screen. The current is 26.4 ma and the phase angle is 78° as shown in Figure 27b, giving a value for the conductance of $6.25 \times 10^{-4}/\Omega$. Thus a change of 9 in PC layer conductance results in a brightness change of about 180 (from 0.01 ml to 1.8 ml at saturation).

36. The linear variation in emittance with frequency at high X-ray intensities as shown in Figure 17 verifies equation (6) which predicts this behavior. The reduction in brightness shifting to lower and lower frequencies as the X-ray intensity decreases is more difficult to explain. The decrease in conductance of the PC layer in addition to the variation in capacitive reactance of both layers probably accounts for this brightness variation but a quantitative analysis was not attempted.

37. A considerable gain in brightness and contrast can be realized over the standard fluorescent screen and the NaI crystal although the screen operation is limited to the X-ray intensity range given by Table II. Unfortunately maximum brightness and contrast do not occur at the same frequency. Since contrast increases with frequency while maximum brightness shifts to lower frequencies as the X-ray intensity decreases, a choice of the operating frequency must be a compromise based upon the requirements of the object to be inspected. For thin low contrast objects a high operating frequency should give good results. For thick objects of medium to high contrast, a low operating frequency is advised.

38. The decay of screen brightness as shown in Figures 22 to 24 varies not only with frequency but with X-ray energy. The decrease in decay time with increasing frequency may be explained by the recombination process which occurs during field reversal. As the frequency of the field reversal increases, the recombination and hence decay rate increases. The reason for the increase in decay time at higher X-ray energies is not known.

CONCLUSIONS

39. The solid state image intensifier screen offers high contrast and brightness over a wide X-ray intensity range. A brightness gain of 25 over the standard fluorescent screen is possible at low energies. A gain greater than five was obtained for the screen when compared with the NaI crystal at the higher energies (2000 kvp and 10 Mev).

40. Screen no. 251 exhibits high brightness with moderate contrast while screen no. 255 has high contrast with brightness comparable to the standard fluorescent screen. Both screens must be operated over a limited X-ray intensity range due to the S-shaped response curve. It may be possible to overcome this limitation by layer formulation and design changes.

41. The screen brightness is a linear function of the frequency at high X-ray intensities. At a given transition point the brightness no longer increases but decreases as the X-ray intensity level is reduced. This transition point shifts toward lower frequencies with a reduction of X-ray intensity. Since brightness and contrast do not occur at the same frequency, a compromise frequency must be chosen depending upon the object to be inspected. A shift to the lower frequencies is advised when the X-ray intensity is low.

42. Two possible solutions to this problem have been suggested.[8] One is the use of frequency modulation to linearize the operating characteristics of the screen. The resulting over-all characteristic would then be an envelope of the individual characteristics. The other solution would be a series combination of two screens with a low frequency applied to the input stage and a high frequency applied to the output stage. This would combine input sensitivity with a high output level, but definition would be adversely affected. Investigation of these methods required the development of a frequency modulated audio-generator and fabrication of a special screen. The long decay time may be of use in medical fluoroscopy and industrial photofluoroscopy however. Two methods of quenching have been proposed, infrared and the Kazan method of erasure. Previous work has shown that infrared exposure did not noticeably hasten the decay.[9] The Kazan method of erasure employs an evaporated layer on top of the PC layer. Then an a-c voltage is applied with a dc bias. Erasure is accomplished by reversing the d-c polarity. A screen with this extra layer was not available for evaluation.

43. Sensitivity was not determined for these screens. However, image quality was affected at low brightness levels by uneven emission from the EL surface. Larger screens are being constructed in an effort to overcome this problem; these screens will be evaluated upon completion.

44. The decay curves of both screens show very long decay times although screen no. 255 is about six times faster than screen no. 251. This feature restricts the use of these screens to inspection of stationary objects.

REFERENCES

1/ Contract NOrd 18369 - Development of a High Brightness, High Resolution Fluoroscopic Screen, U. S. Radium Corporation, November 1959

2/ Zalm, P - The Electroluminescence of ZnS Type Phosphors, PHILIPS RESEARCH REPORTS, Dec 1956, p 6

3/ Op.cit. p 10

4/ Op. cir. p 22

5/ Diemer, et al - Solid State Image Intensifier, PHILIPS RESEARCH REPORTS, 10 Dec 1955, p 405

6/ Op. cit. p 406

7/ Op. cit. p 421

8/ Ref 5/ p 412

9/ Solid State Image Intensifier for Industrial Applications, Third Quarterly Report, September 13, 1959 - December 13, 1959. Contract DA-36-034-ORD-2856RD, p 7

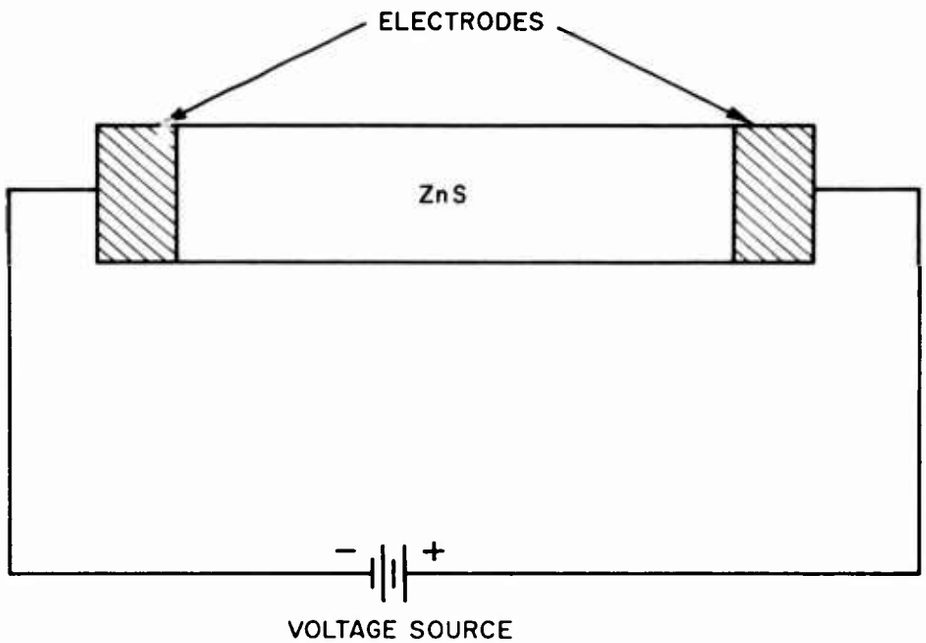

FIG. 1 ZnS CRYSTAL EXCITATION

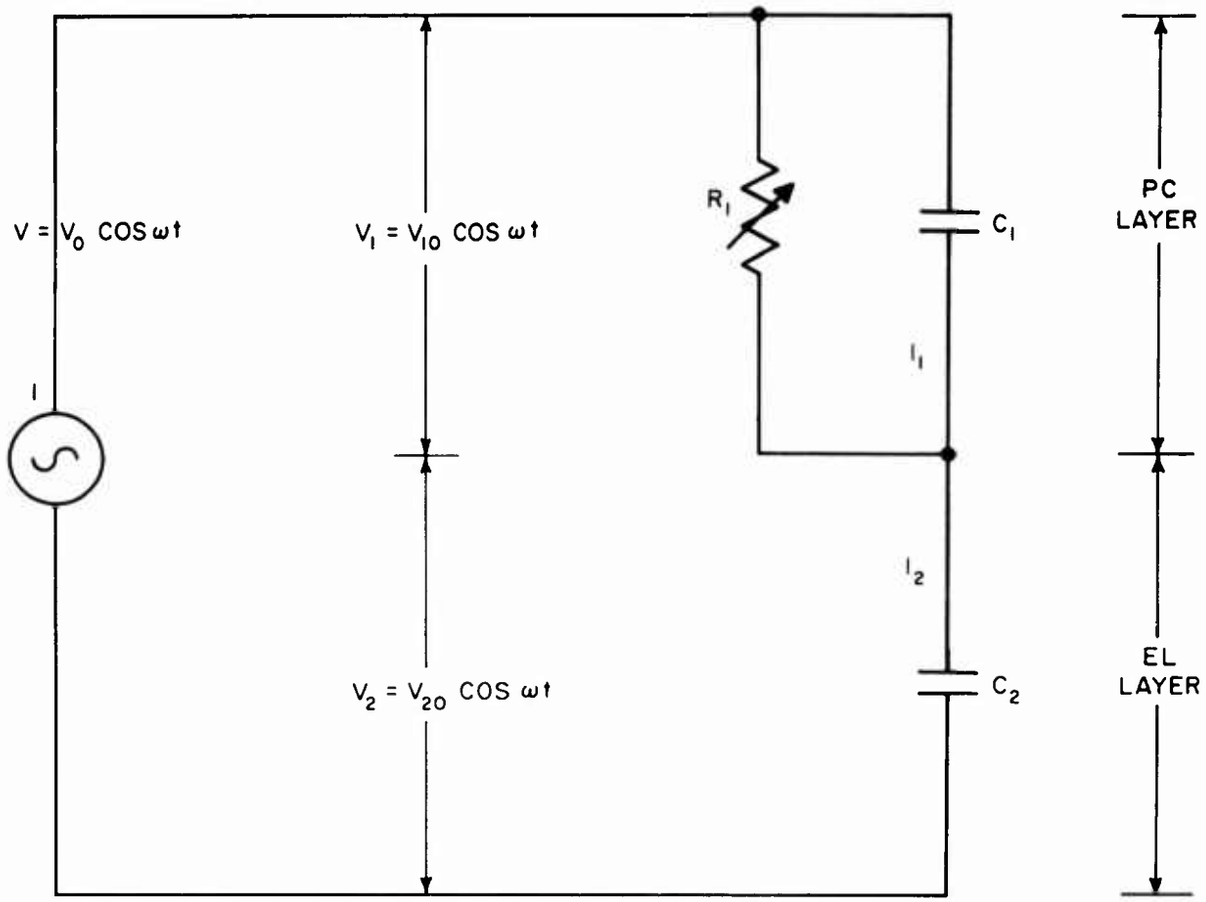

FIG. 2 EQUIVALENT ELECTRICAL CIRCUIT OF THE PC-EL LAYER COMBINATION

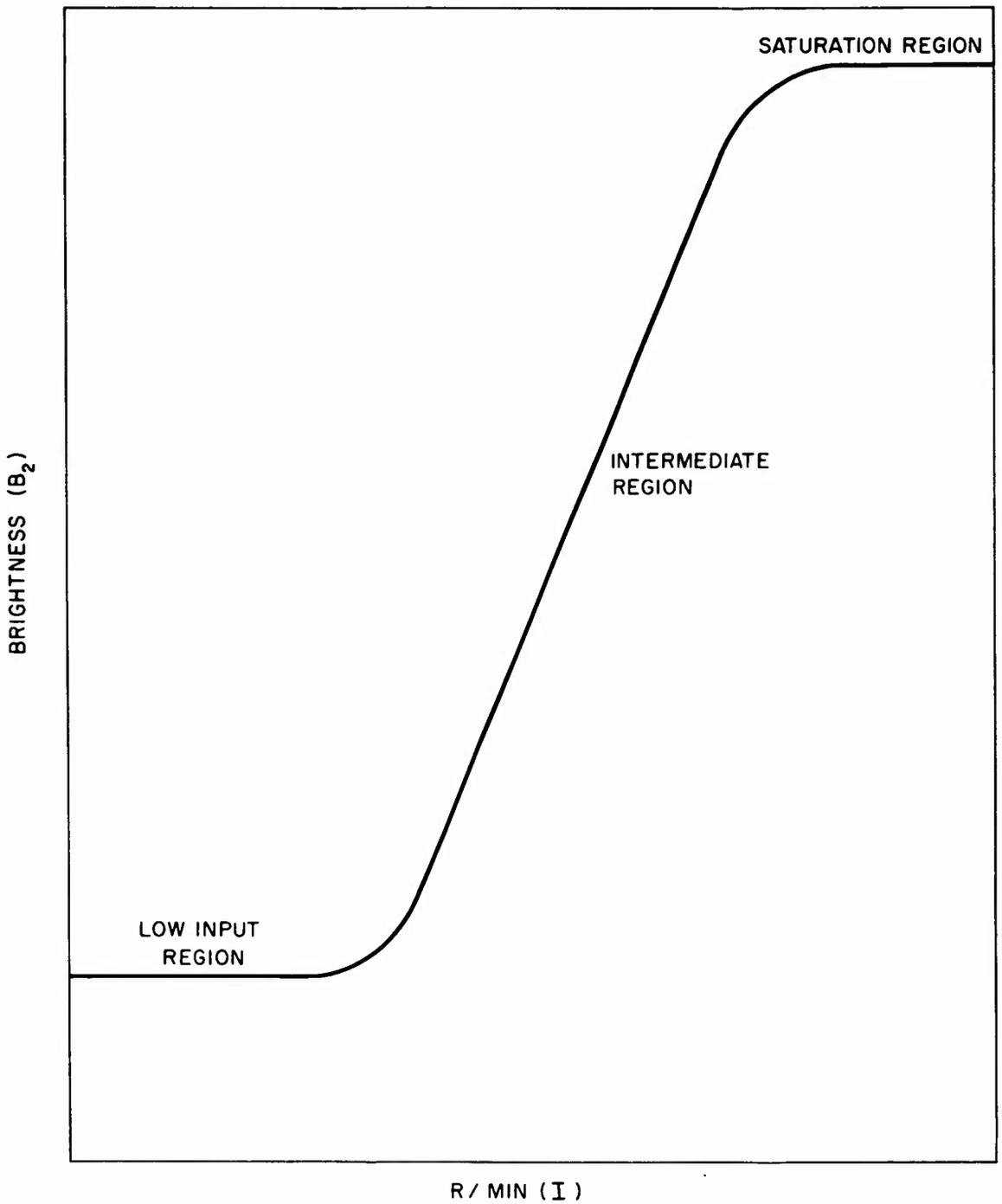

FIG. 3 THEORETICAL RESPONSE CURVE FOR A SOLID STATE INTENSIFYING SCREEN

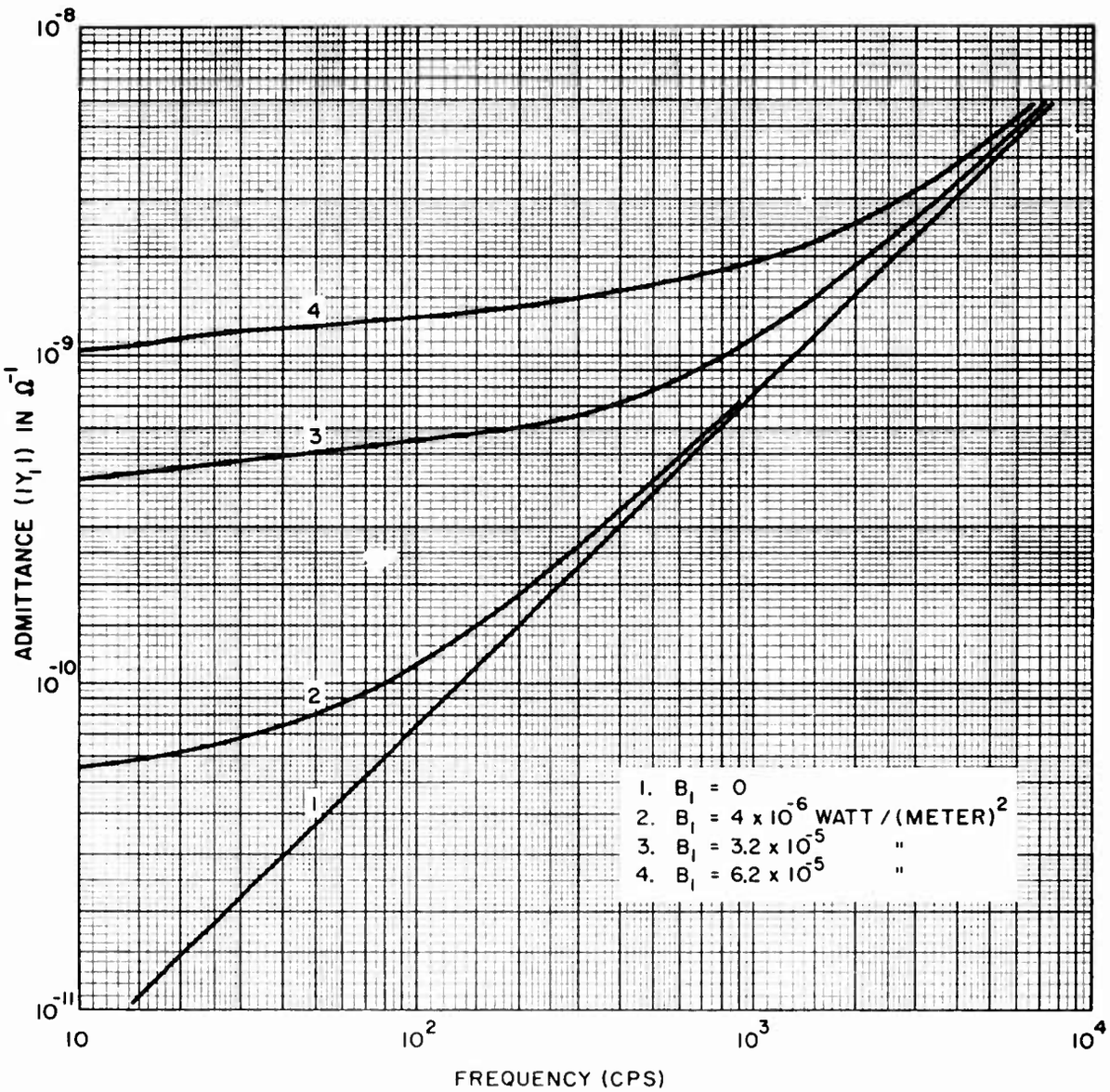

FIG. 4 ADMITTANCE OF Cd S AS A FUNCTION OF FREQUENCY AT VARIOUS INPUT INTENSITY LEVELS

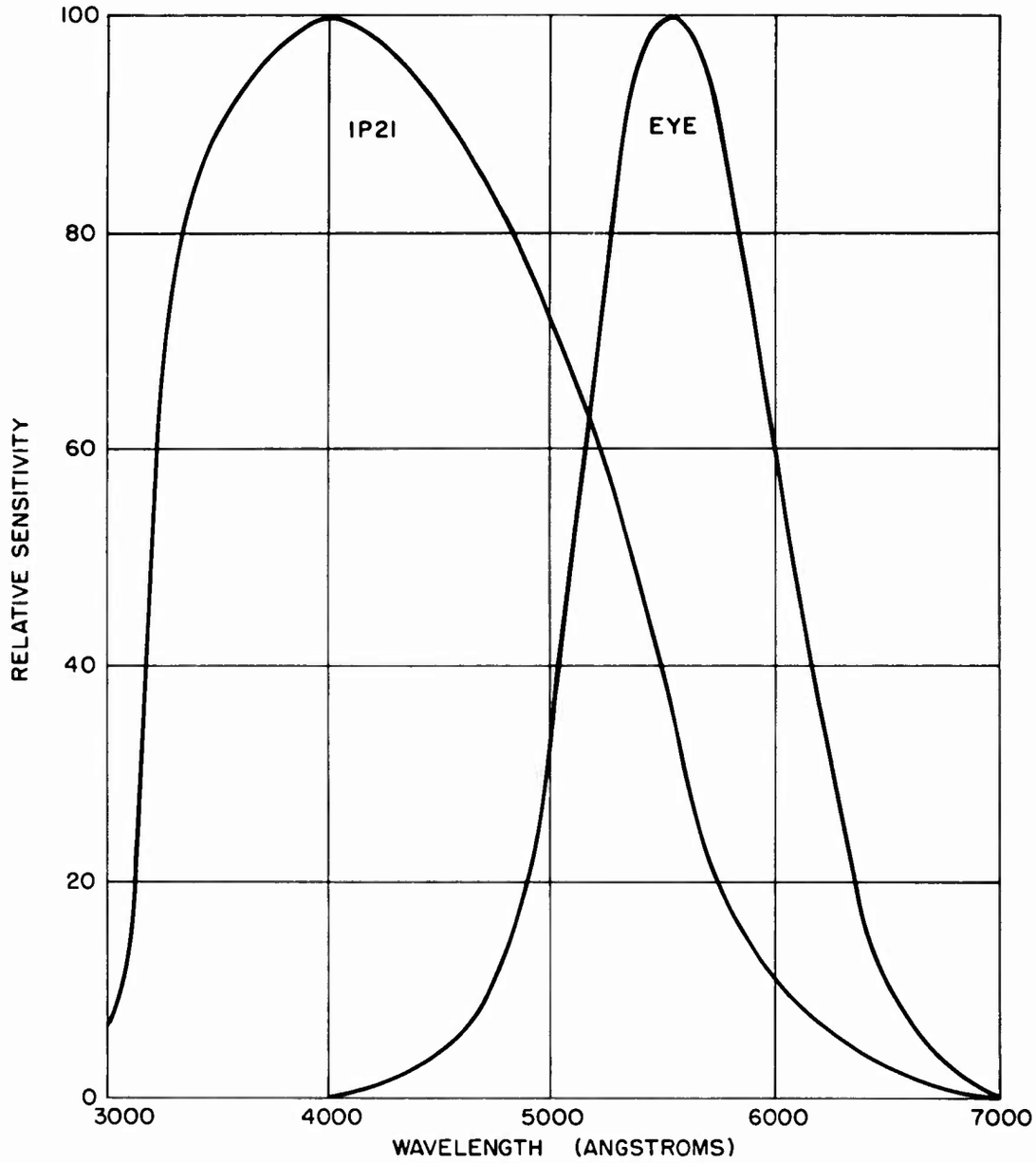

FIG. 5 SPECTRAL SENSITIVITY CHARACTERISTICS OF A IP21 PHOTOTUBE AND THE HUMAN EYE (TO EQUAL VALUES OF RADIANT FLUX AT ALL WAVELENGTHS)

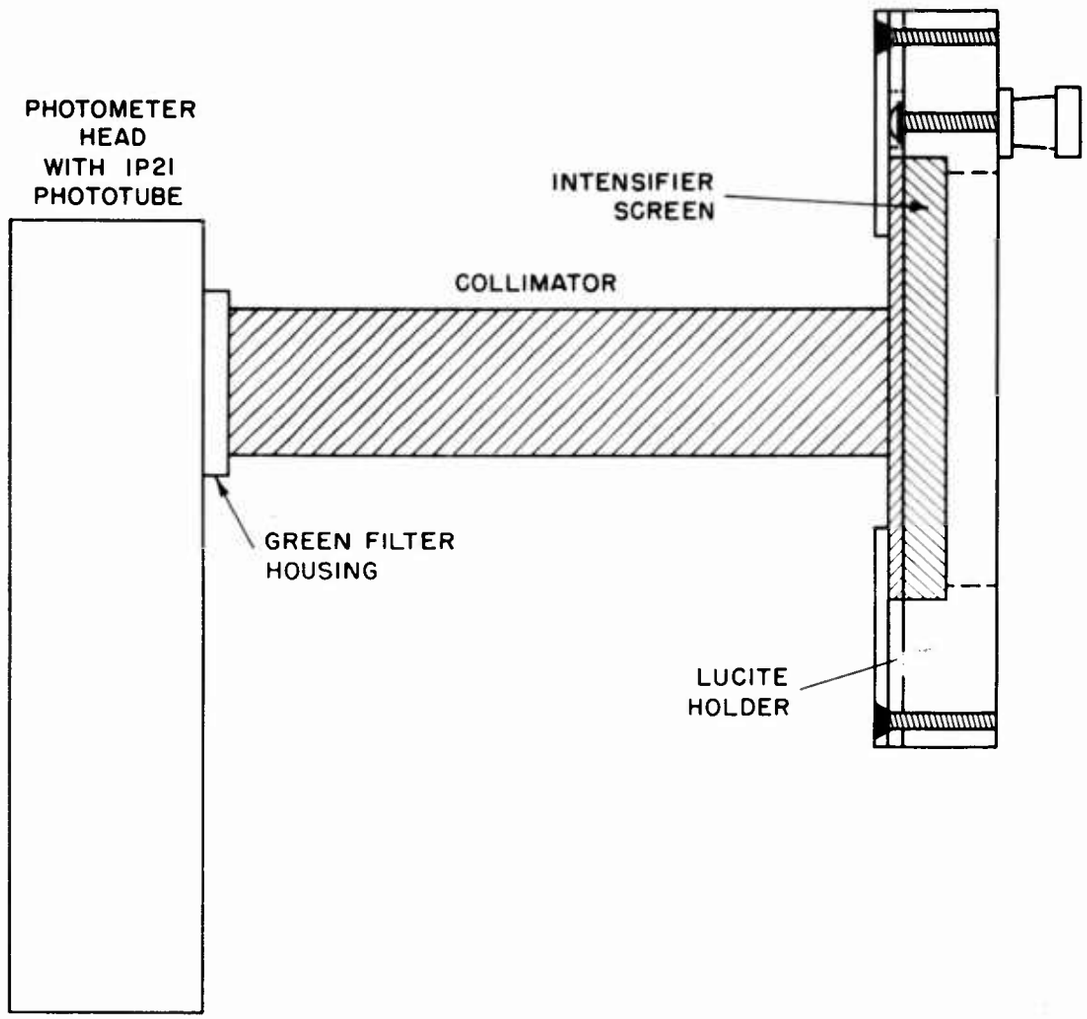

FIG. 6 DIAGRAM OF SCREEN HOLDER AND PHOTOTUBE COLLIMATOR

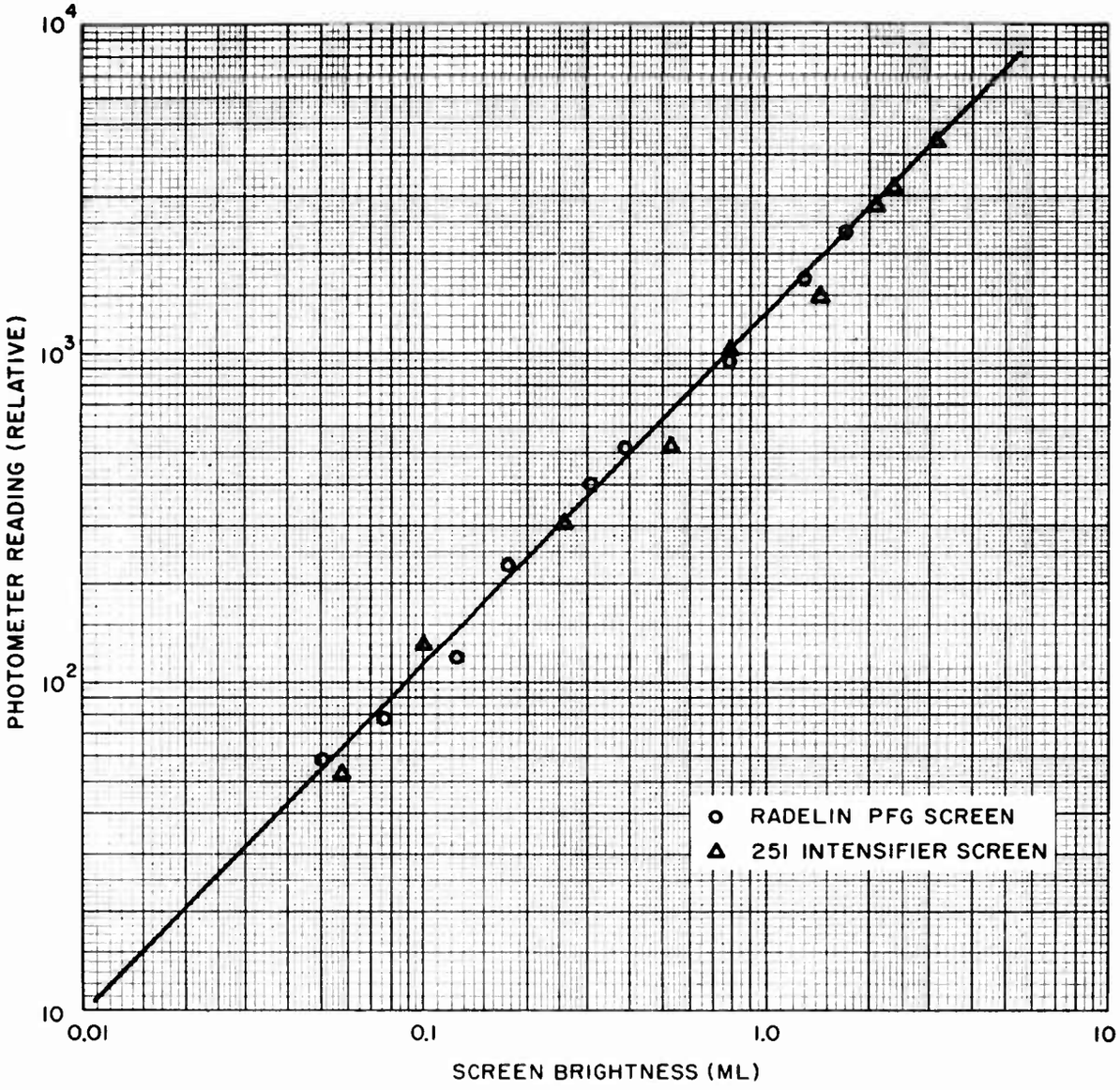

FIG. 7 PHOTOMETER CALIBRATION CURVE

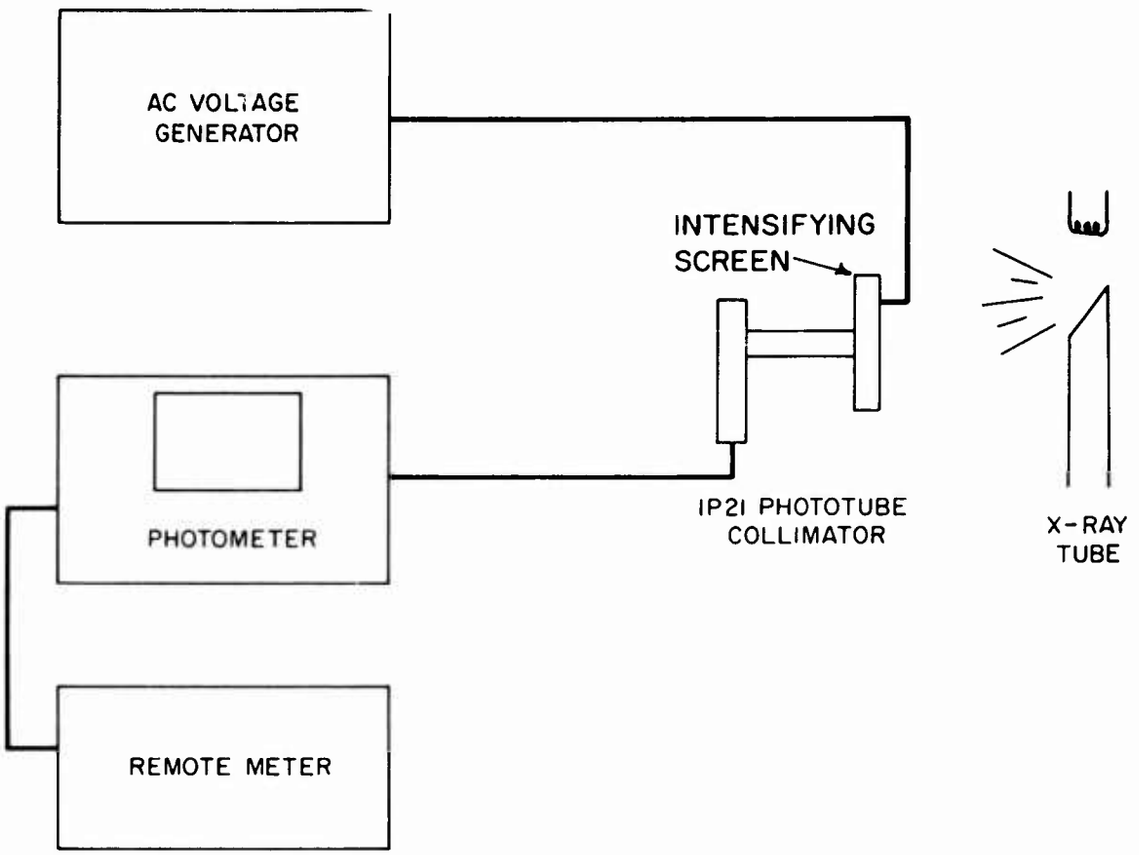

FIG. 8 DIAGRAM OF EXPERIMENTAL SET-UP

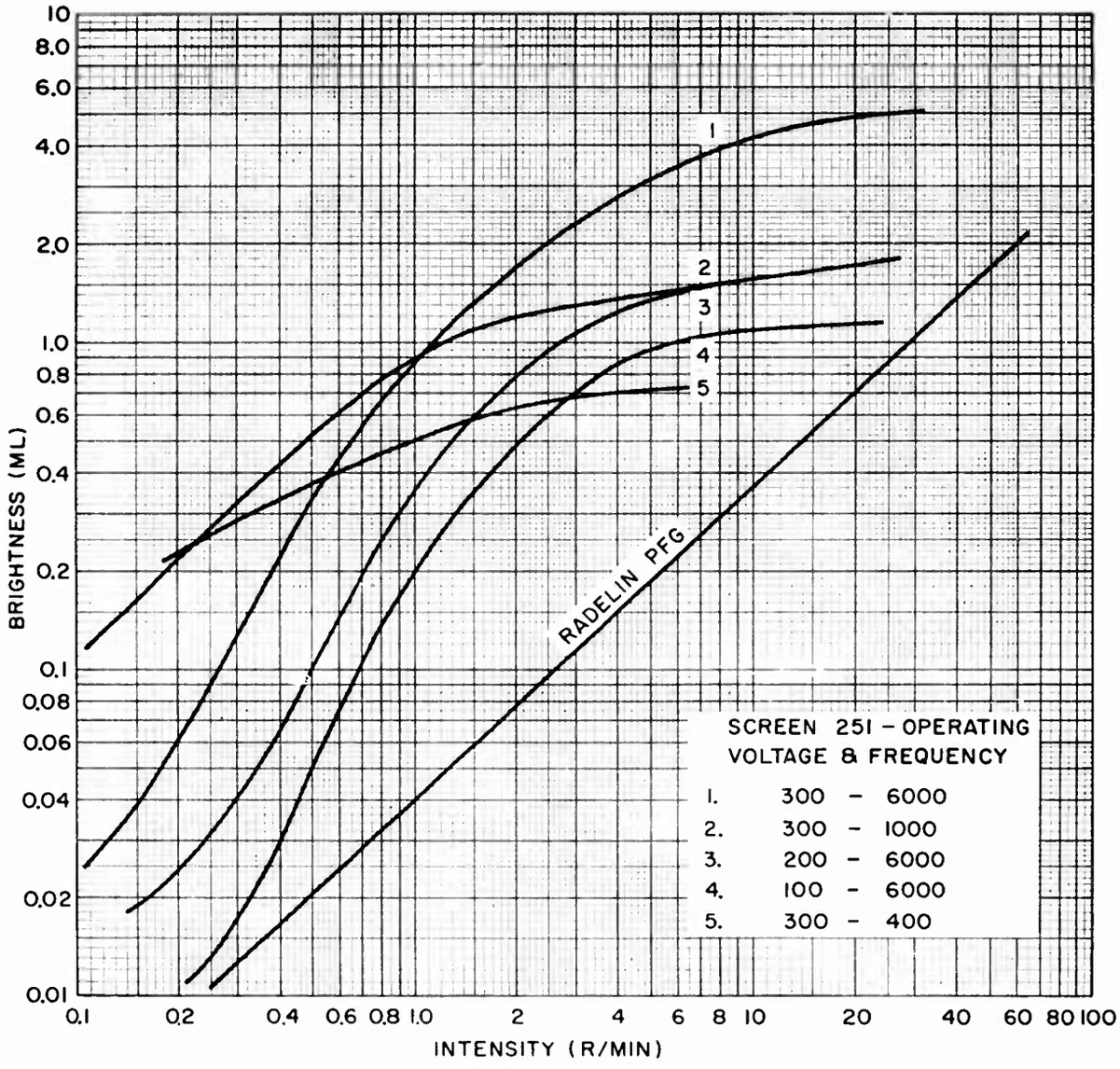

FIG. 9 BRIGHTNESS RESPONSE CURVES FOR SCREEN 251 AT 90 KVP

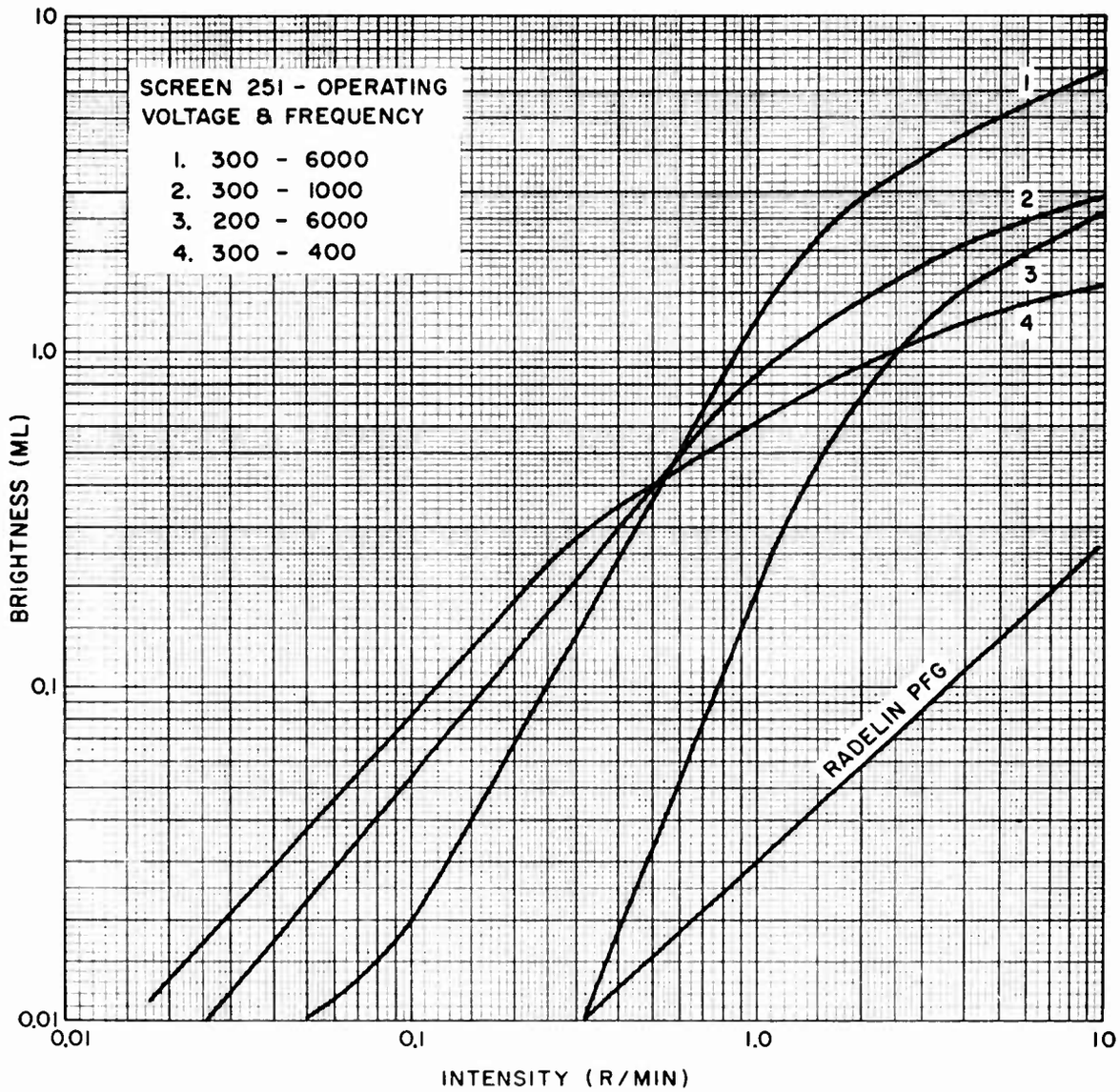

FIG. 10 BRIGHTNESS RESPONSE CURVES FOR SCREEN 251 AT 150 KVP

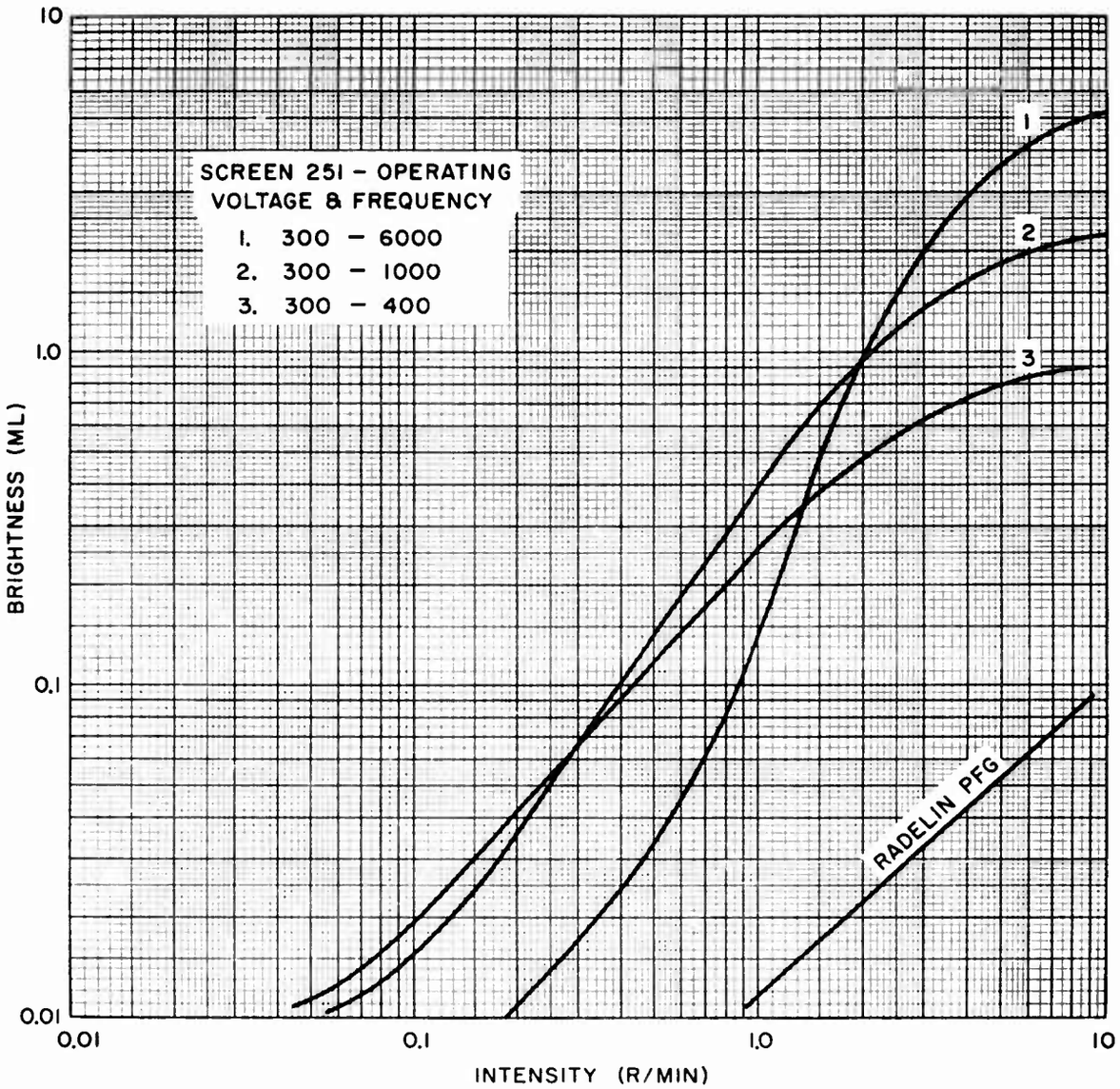

FIG. 11 BRIGHTNESS RESPONSE CURVES FOR SCREEN 251 AT 250 KVCP

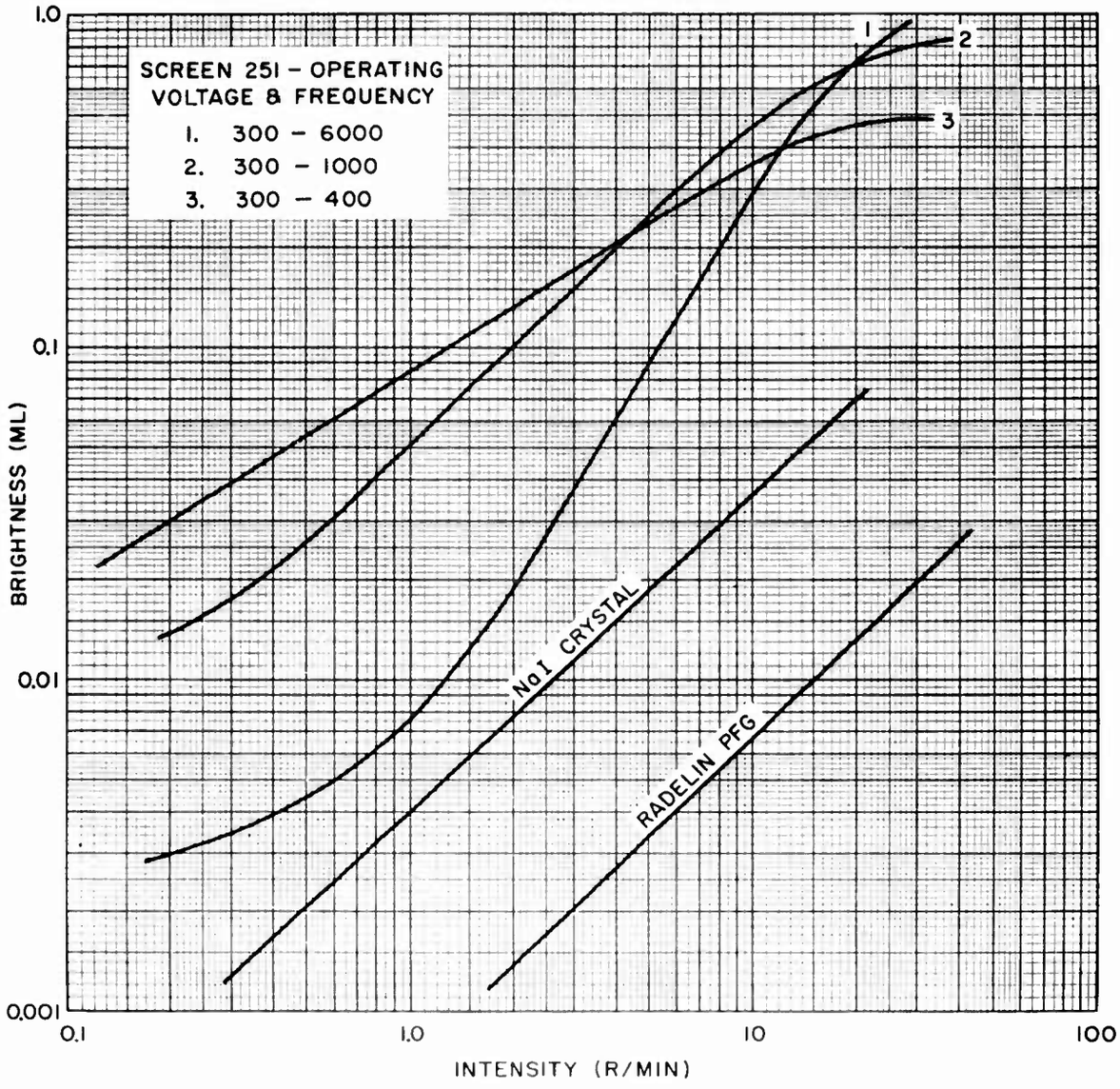

FIG. 12 BRIGHTNESS RESPONSE CURVES FOR SCREEN 251 AT 2000 KVP

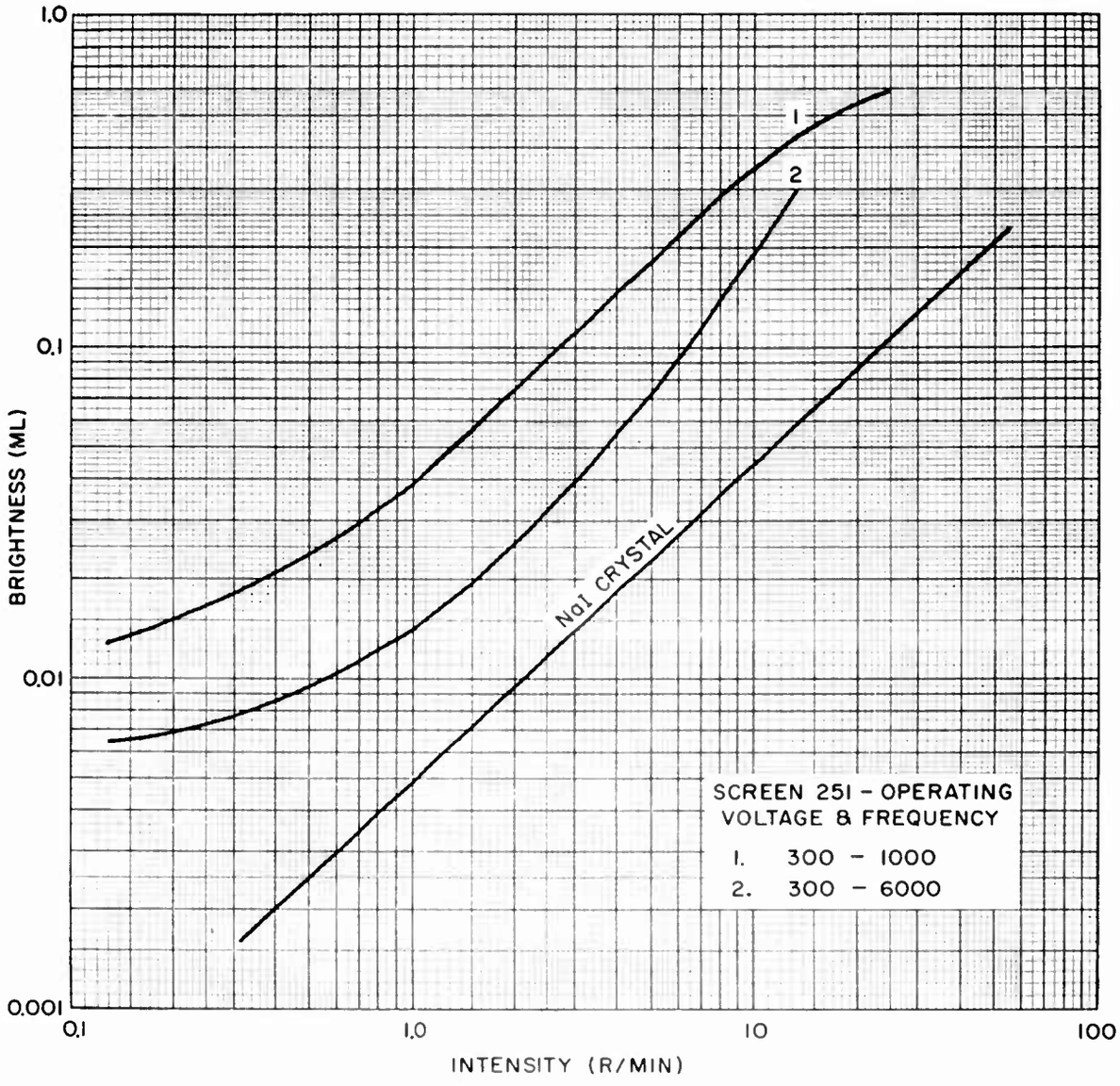

FIG. 13 BRIGHTNESS RESPONSE CURVES FOR SCREEN 251 AT 10 MEV

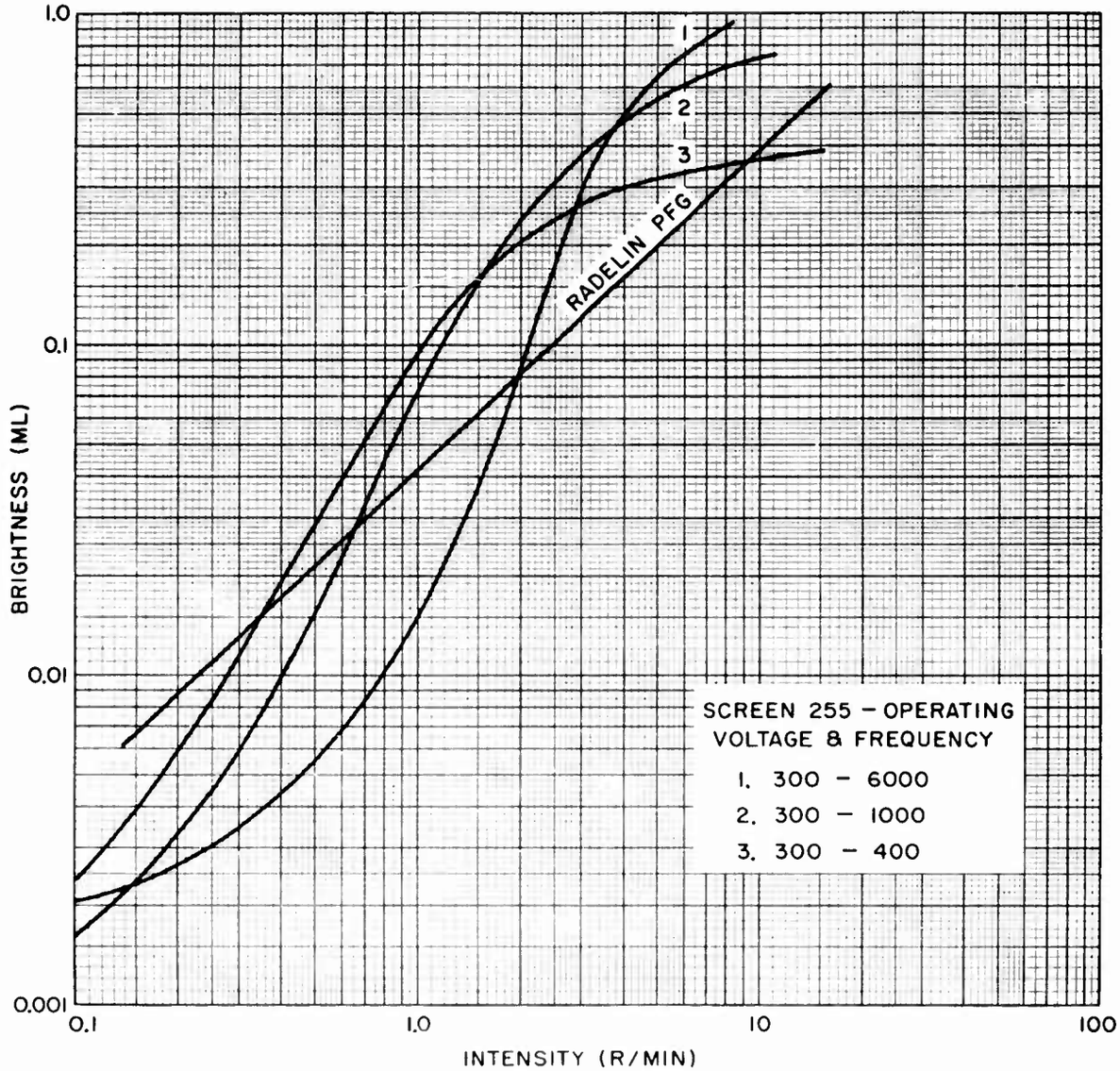

FIG. 14 BRIGHTNESS RESPONSE CURVES FOR SCREEN 255 AT 90 KVCP

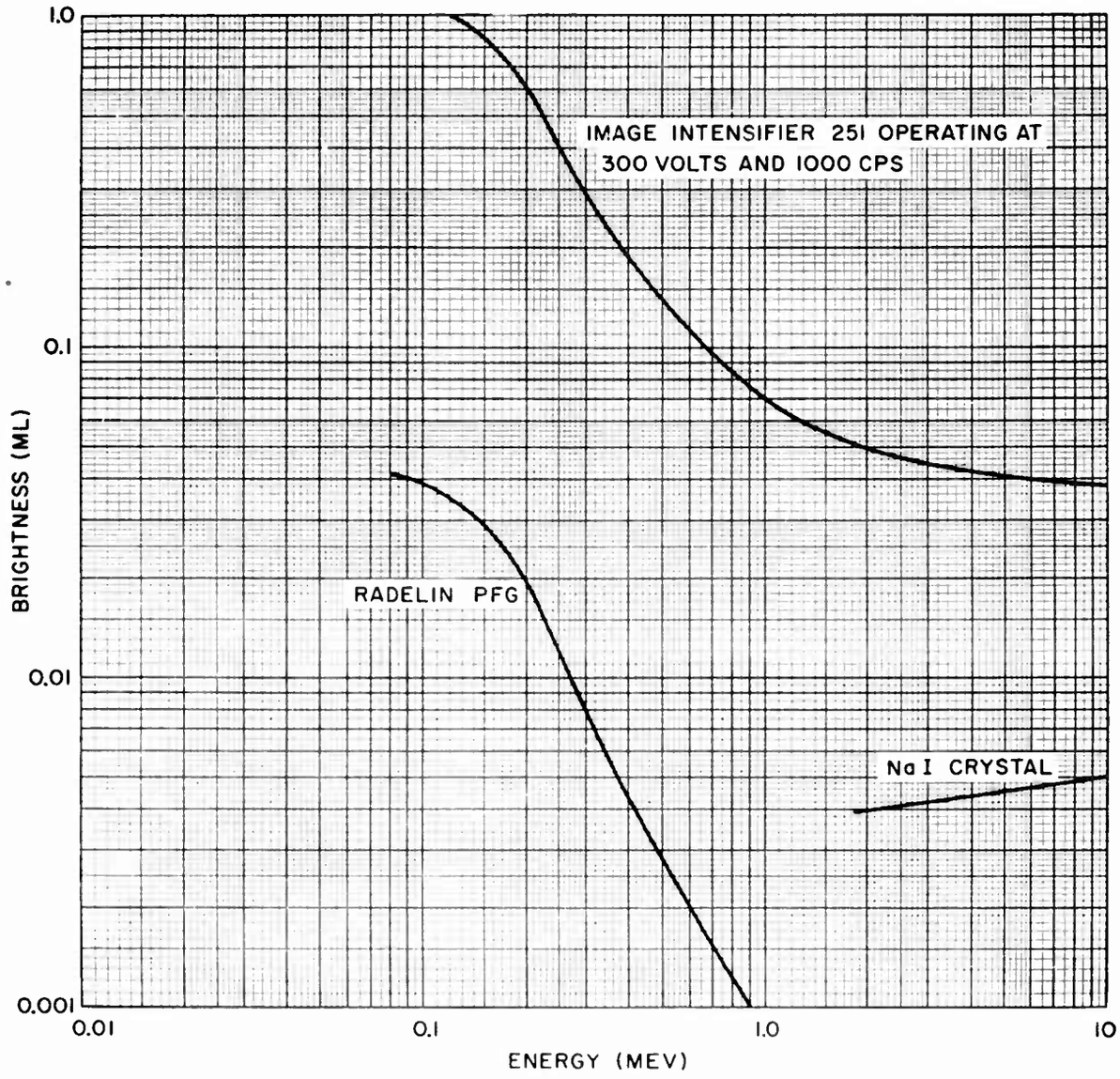

FIG. 15 BRIGHTNESS VS ENERGY FOR INTENSIFIER 251, RADELIN PFG AND NaI CRYSTAL AT 1.0 R/MIN

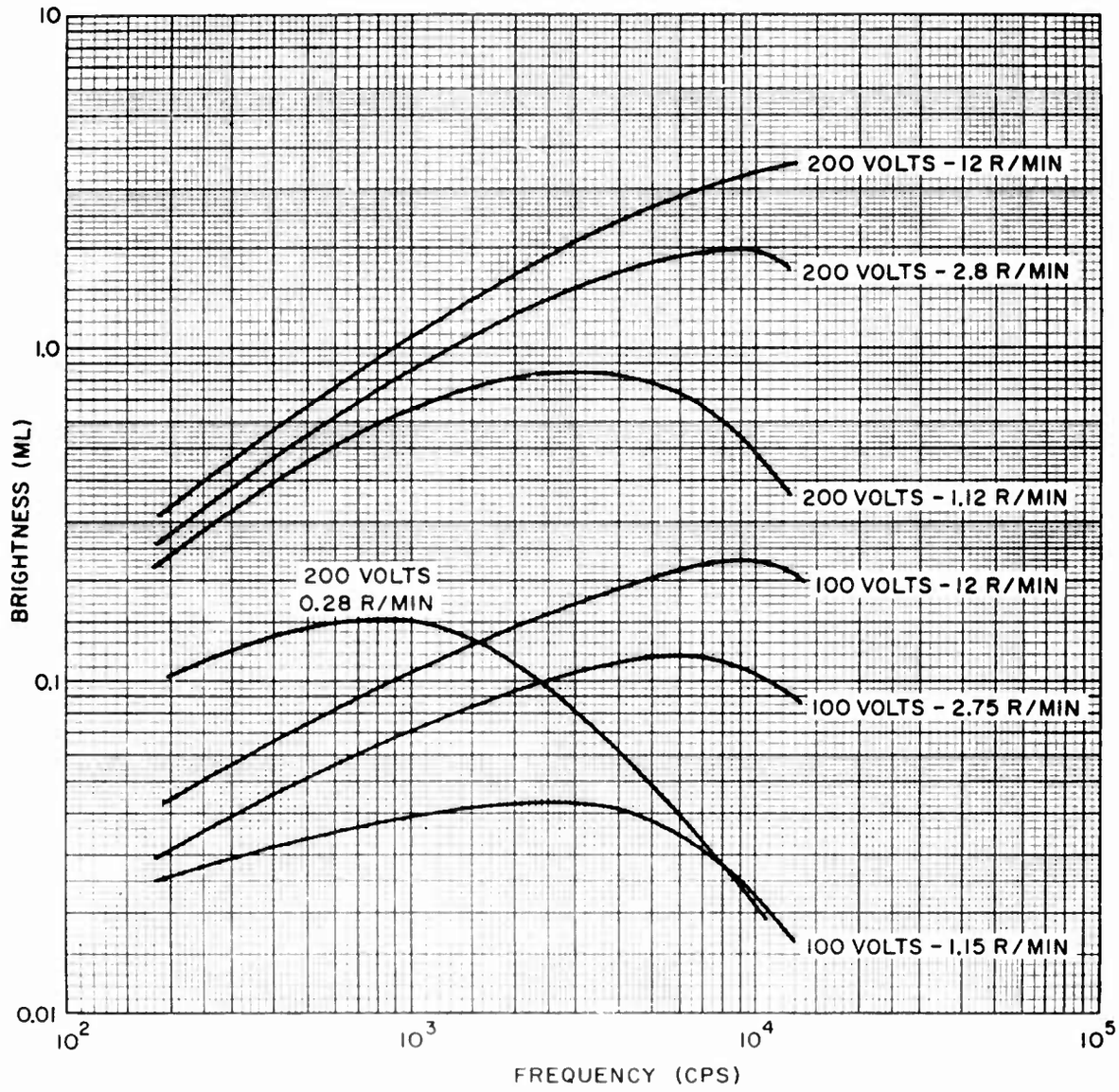

FIG. 16 BRIGHTNESS VS FREQUENCY FOR SCREEN 251 AT 90 KVP

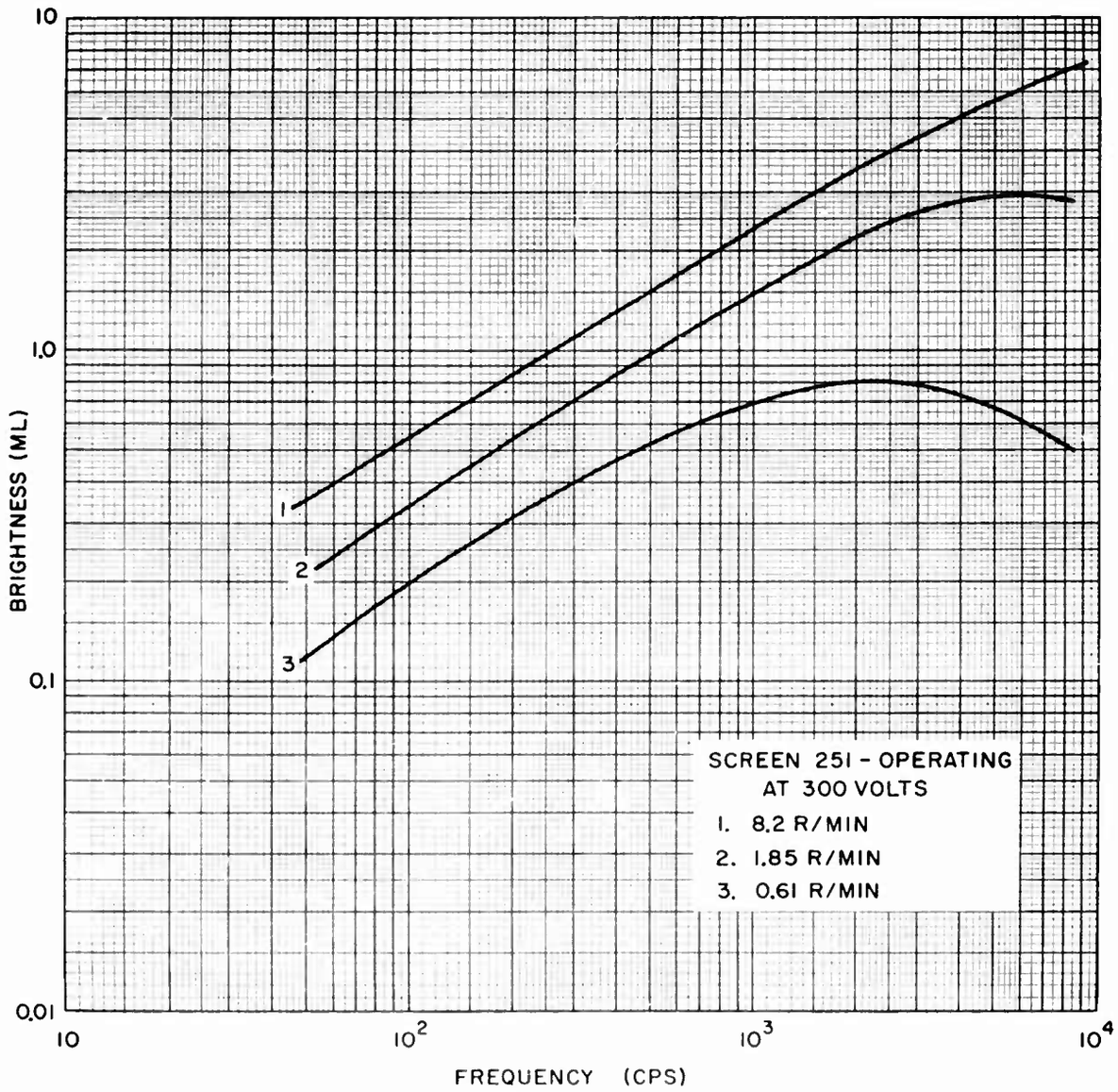

FIG. 17 BRIGHTNESS VS FREQUENCY FOR SCREEN 251 AT 90 KVP

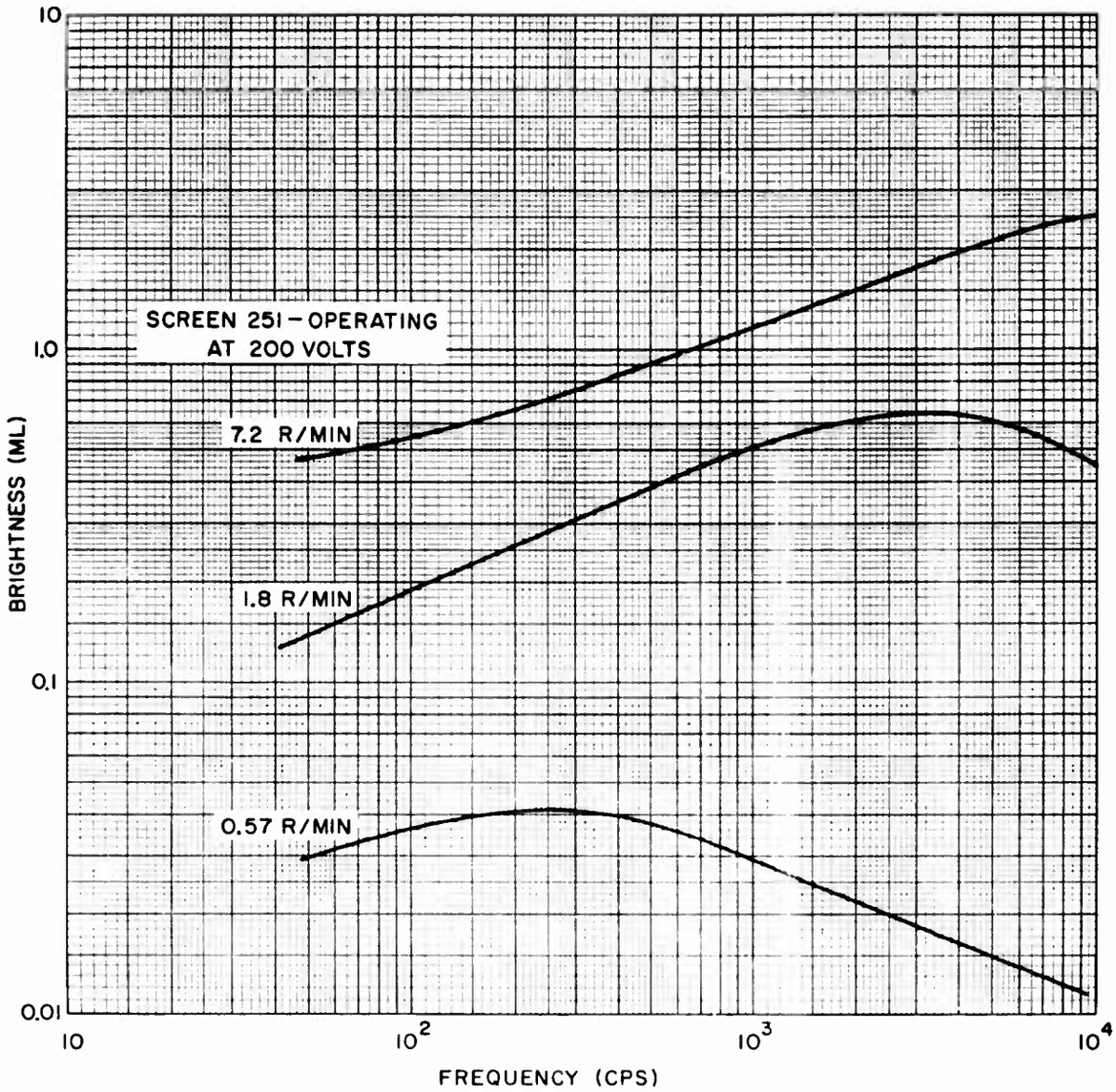

FIG. 18 BRIGHTNESS VS FREQUENCY FOR SCREEN 251 AT 150 KVCP

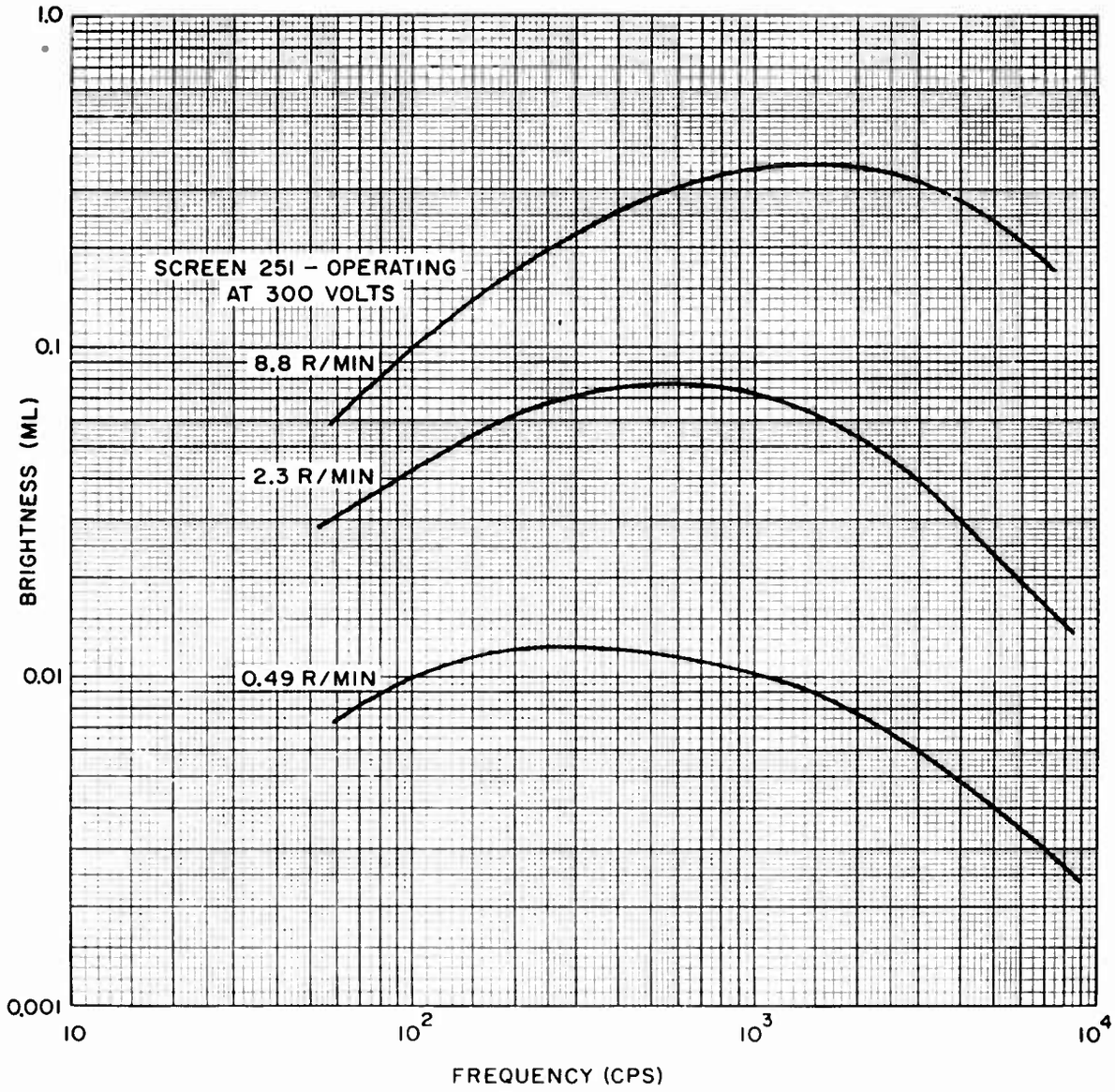

FIG. 19 BRIGHTNESS VS FREQUENCY FOR SCREEN 251 AT 2000 KVP

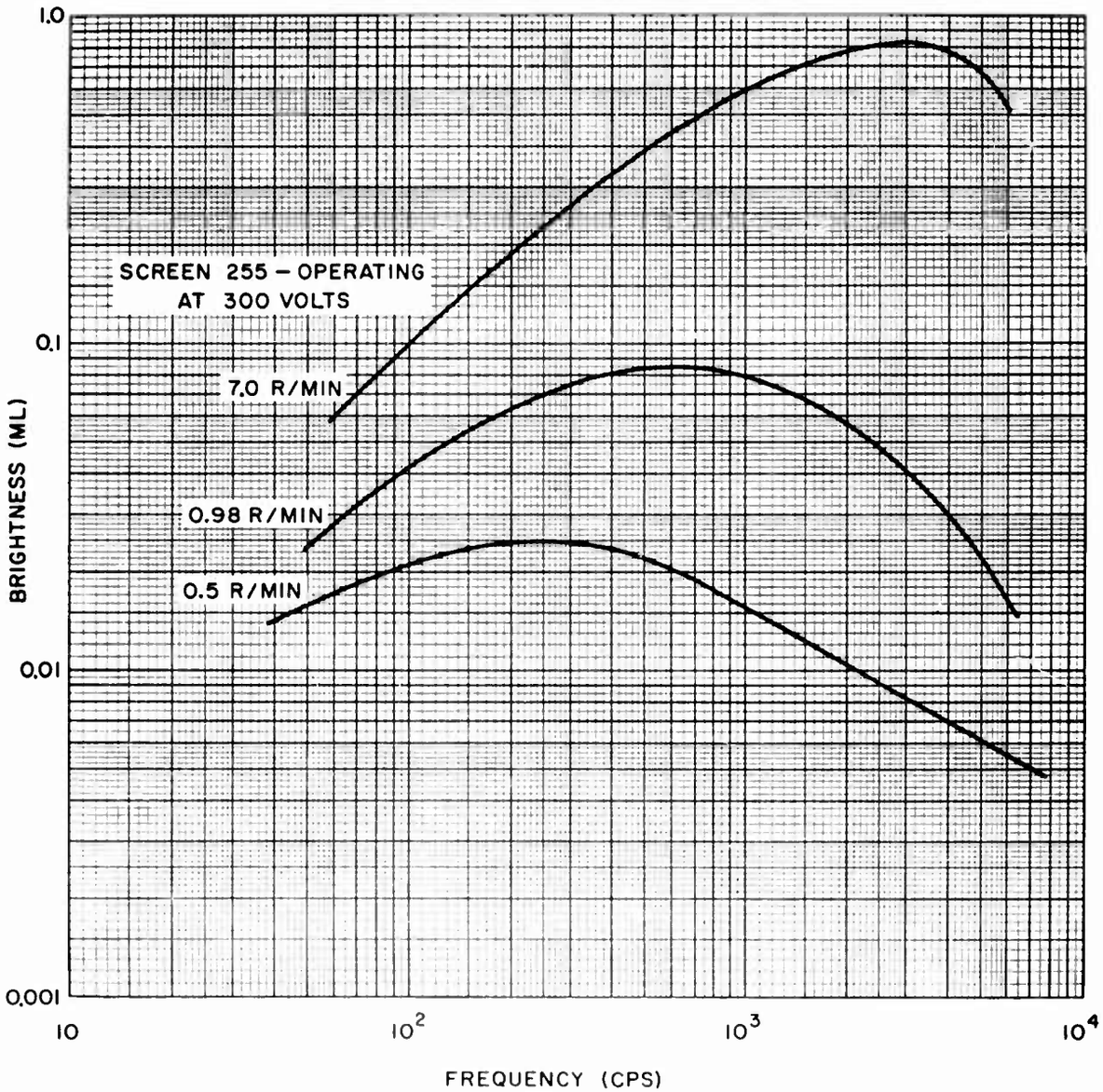

FIG. 20 BRIGHTNESS VS FREQUENCY FOR SCREEN 255 AT 90 KVCP

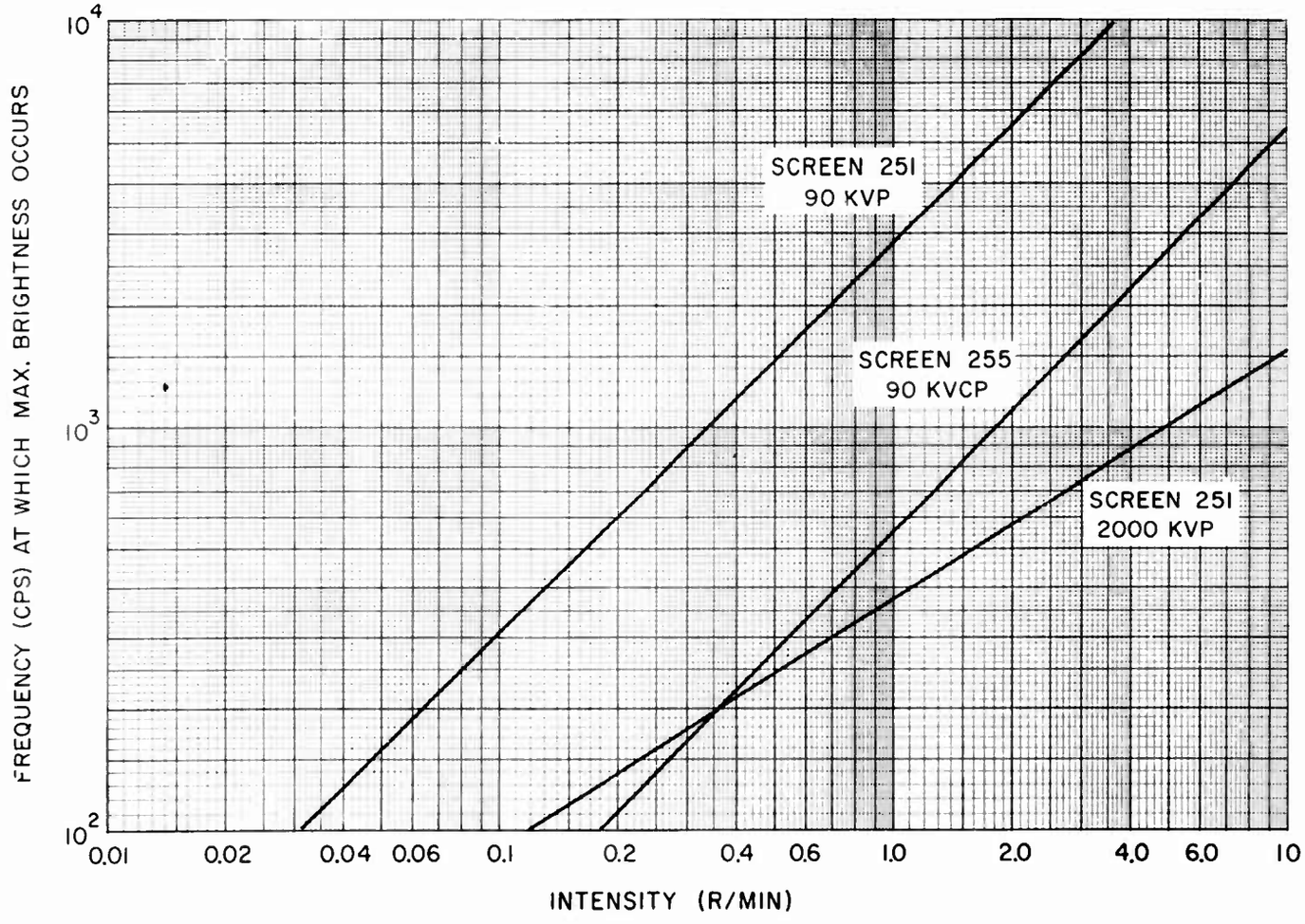

NOLTR 61-115

FIG. 21 FREQUENCY FOR MAXIMUM BRIGHTNESS VS INTENSITY FOR SCREENS 251 AND 255

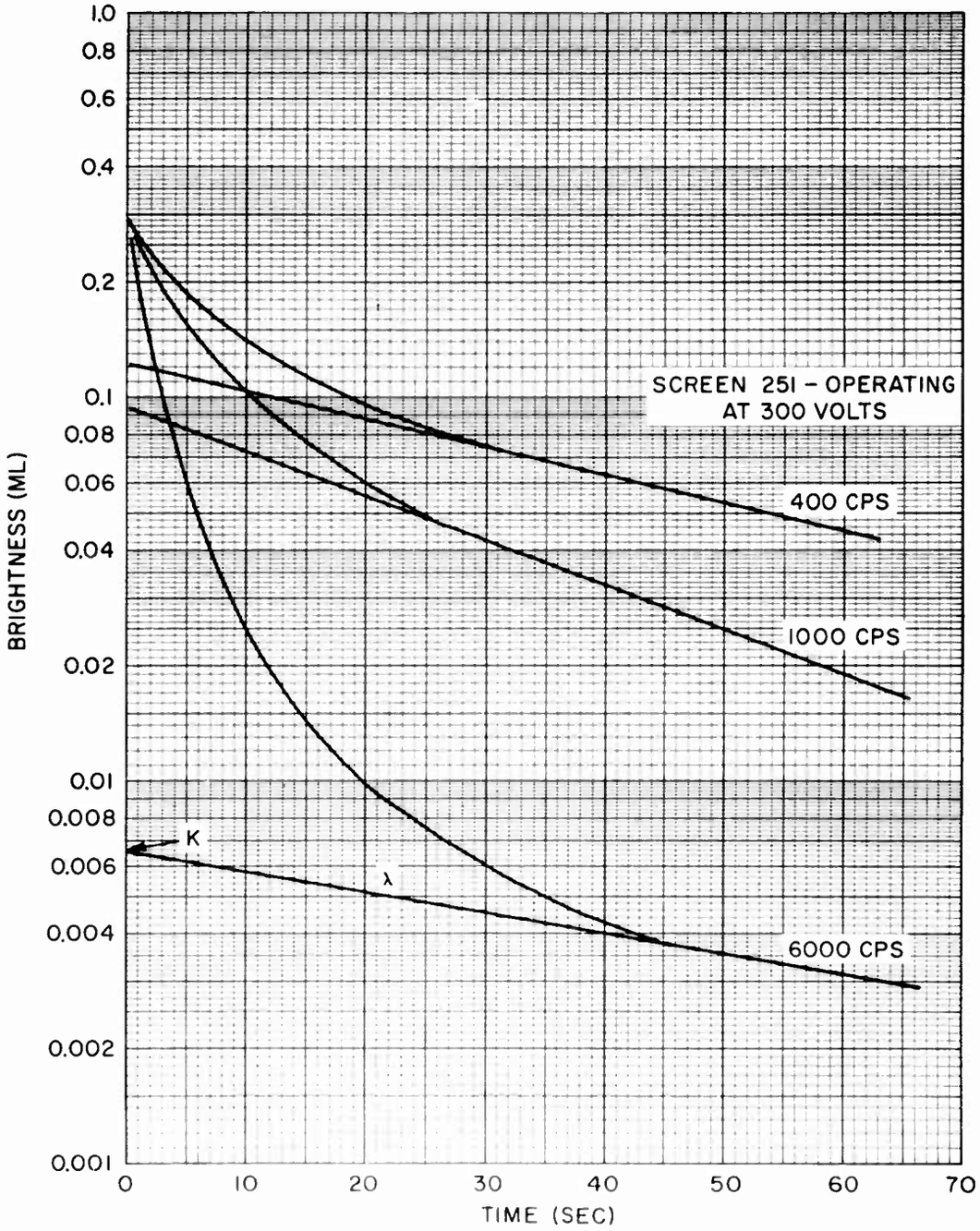

FIG. 22 DECAY CURVES FOR SCREEN 251 AT 90 KVP

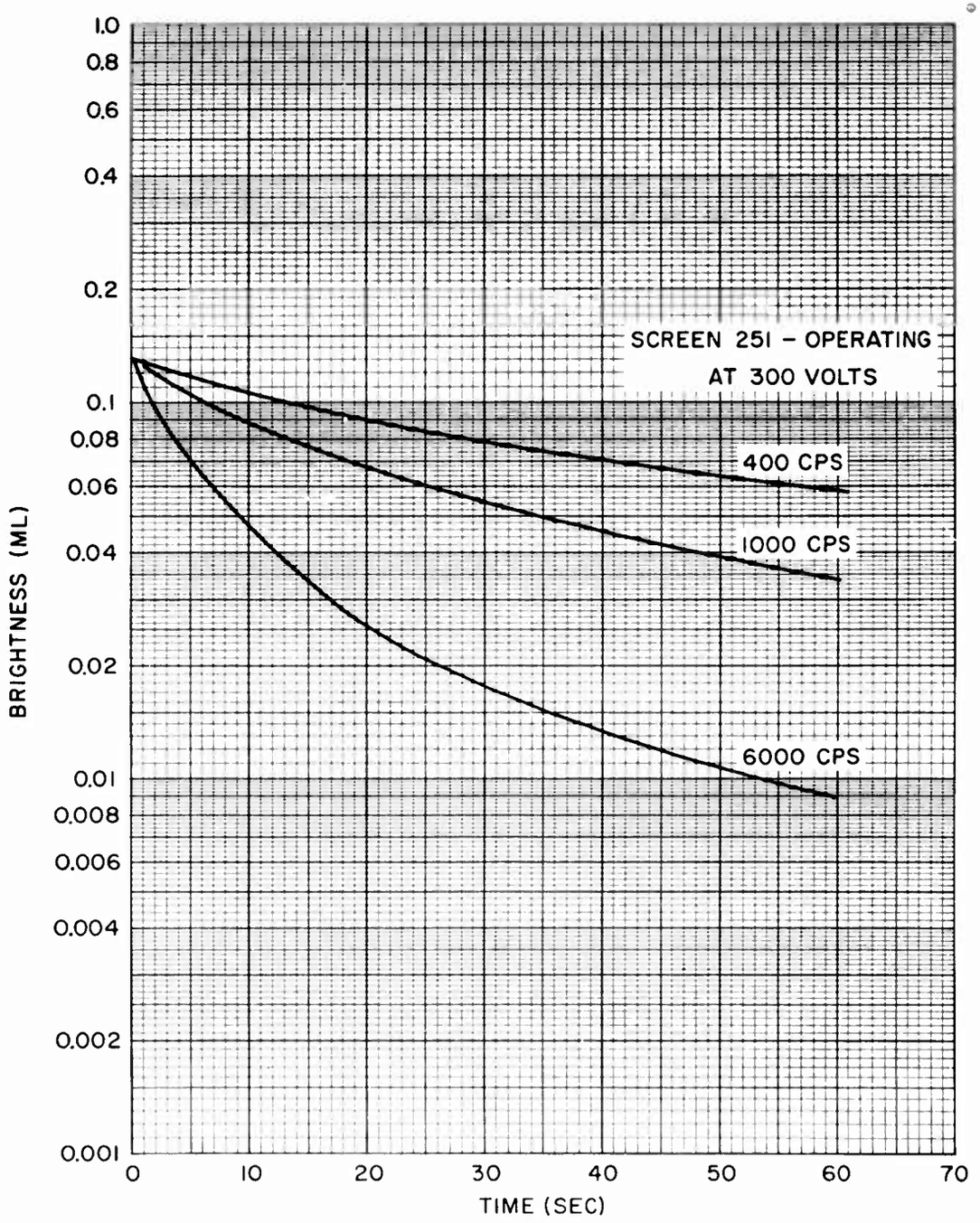

FIG. 23 DECAY CURVES FOR SCREEN 251 AT 2000 KVP

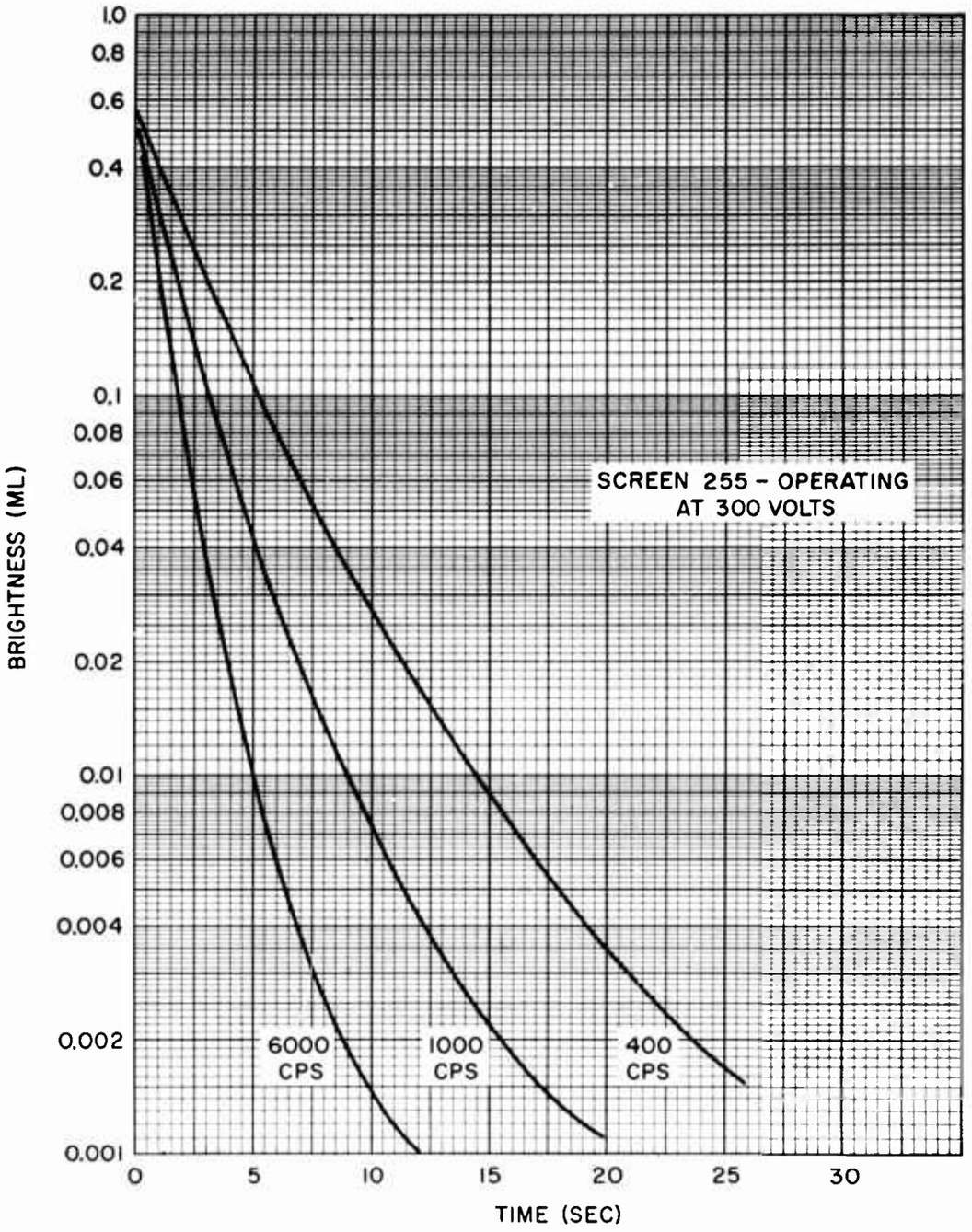

FIG. 24 DECAY CURVES FOR SCREEN 255 AT 90 KVCP

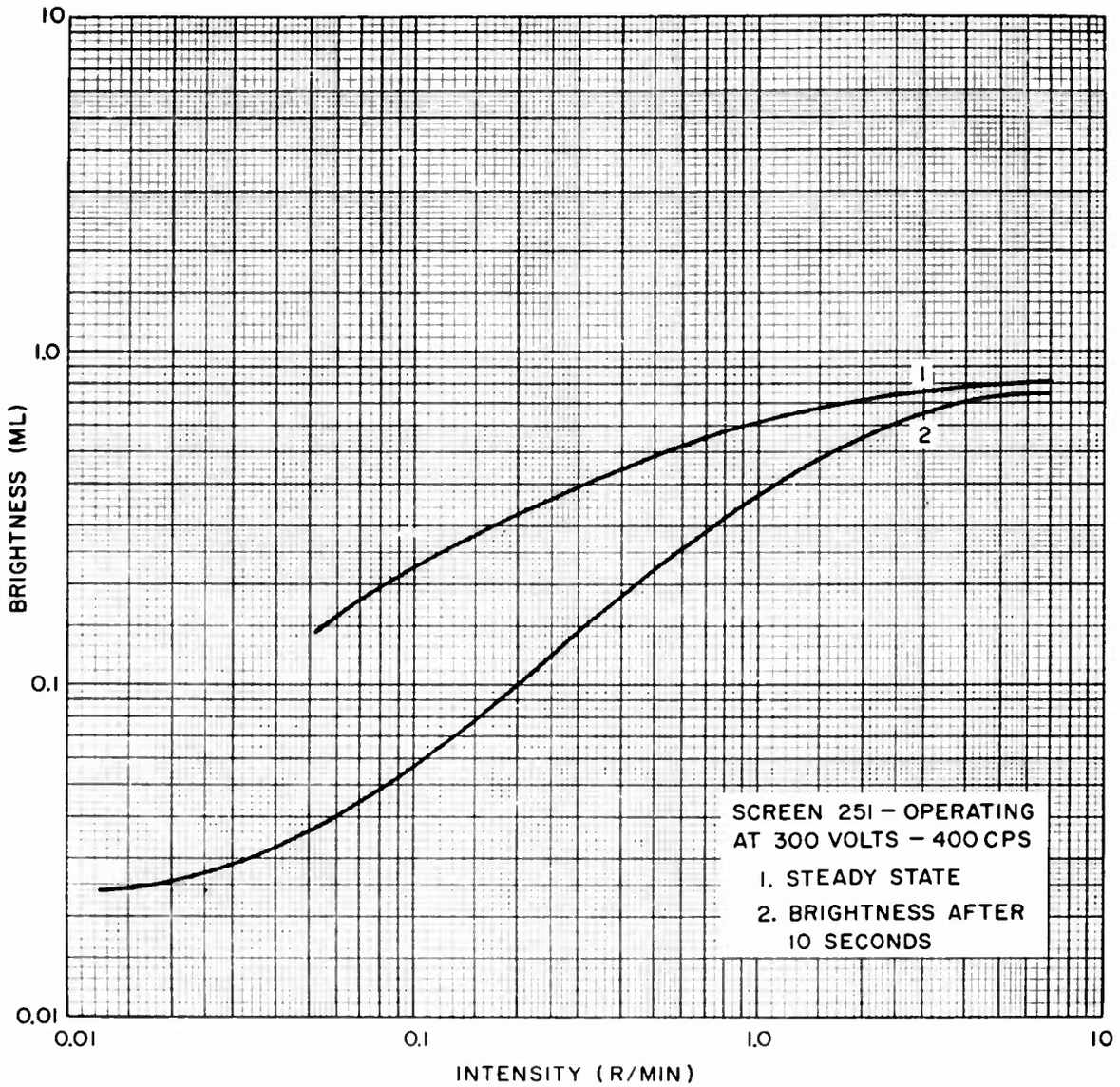

FIG. 25 BRIGHTNESS RESPONSE CURVES SHOWING BUILDUP CHARACTERISTIC OF SCREEN 251 AT 90 KVCP

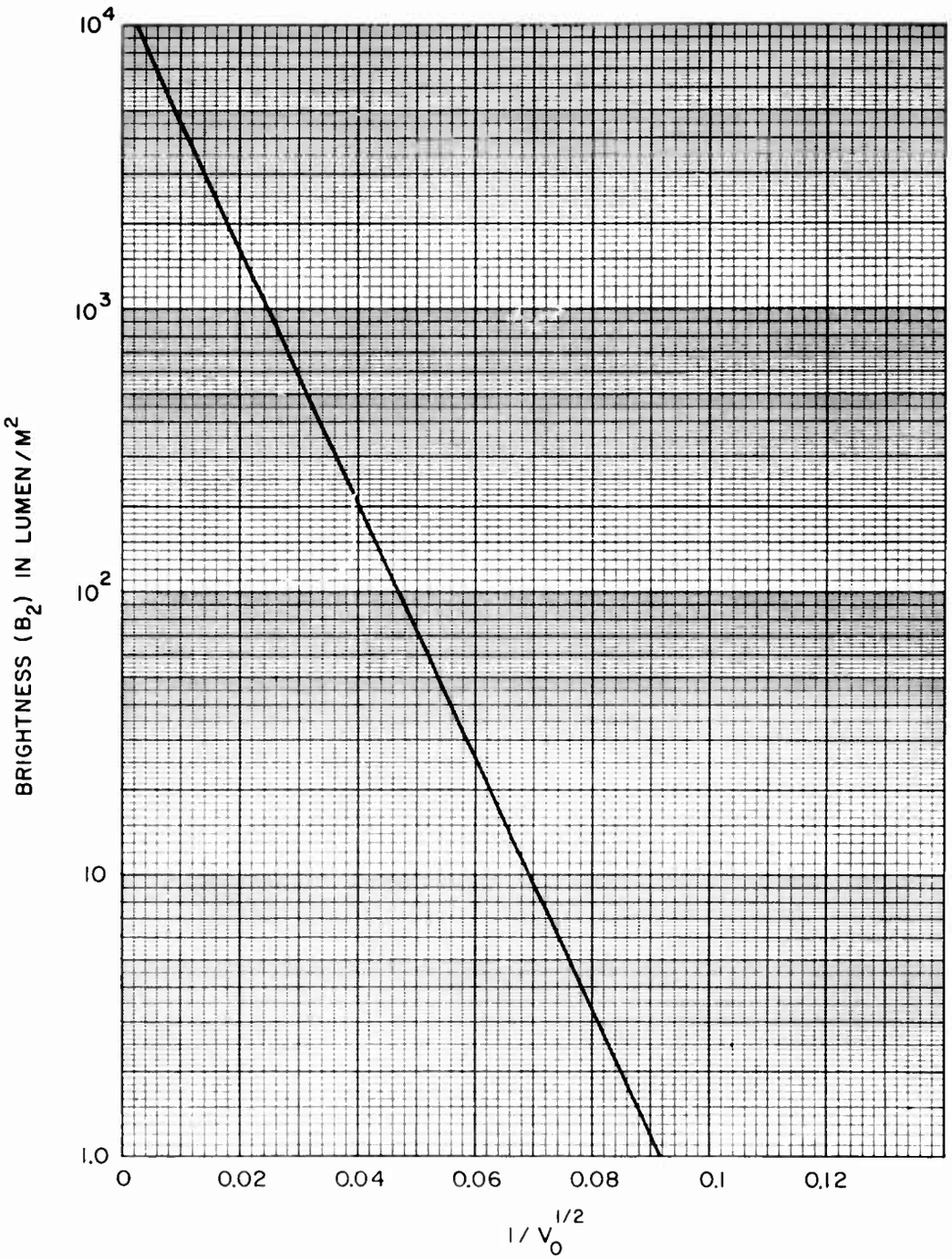

FIG. 26 BRIGHTNESS (B_2) VS $1/V_0^{1/2}$ FOR SCREEN 251 AT 90 KVP – 6000 CPS

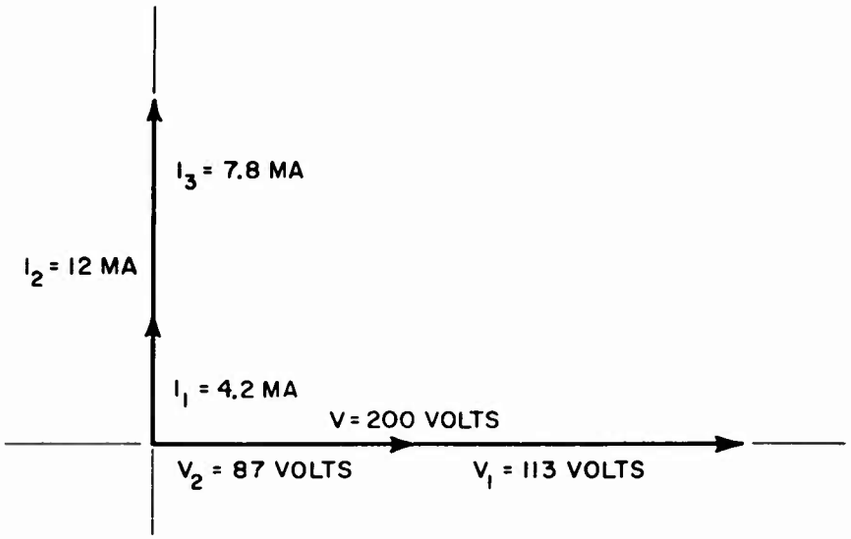

A. 0 R/MIN 6000 CPS

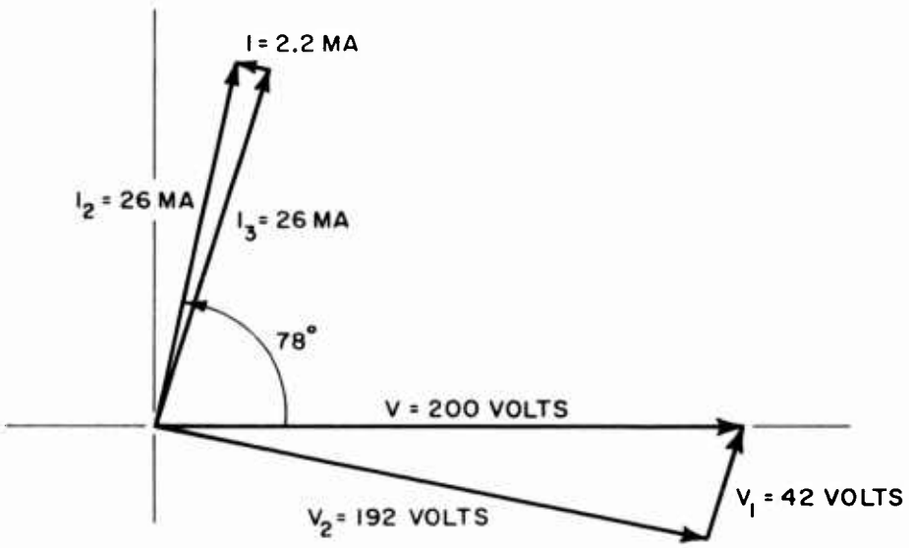

B. 14.5 R/MIN 6000 CPS

FIG. 27 VECTOR DIAGRAM OF THE VOLTAGE AND CURRENT RELATIONSHIPS FOR SCREEN 251

APPENDIX A

A-1. The capacitance of the PC and EL layers of screen no. 251 are calculated using the following formula

$$C = \frac{\varepsilon_o K A_s}{d}$$

where

ε_o = 8.85×10^{-12} farad/m

K = dielectric constant of the layer

A_s = screen area in m^2

d = layer thickness in meters

For the EL layer

d = 5.1×10^{-5}m, K = 5

For the PC layer

d = 3.8×10^{-4}m, K = 10

A_s for screen no. 251 = 42×10^{-4} m^2

The capacitance of the PC layer

$C_1 = 9.8 \times 10^{-10}$ farad

The capacitance of the EL layer

$C_2 = 3.64 \times 10^{-9}$ farad.

APPENDIX B

B-1. Calculation of the PC layer dark conductance G_{1D}

$$B_2 = \omega B_{2\alpha} \exp\left[\frac{-A}{V_o} I/2 \left(\frac{G_{1D}^2 + \omega^2(C_1+C_2)^2}{G_{1D}^2 + {}^2C_1{}^2}\right)^{1/4}\right] \quad (10)$$

is rewritten as:

$$\left(\frac{\ln \frac{B_2}{\omega B_{2\alpha}}}{-\frac{A}{V_o} 1/2}\right)^4 = \frac{G_{1D}^2 + \omega^2(C_1+C_2)^2}{G_{1D}^2 + \omega^2 C_1{}^2}$$

$$\left(\frac{\ln \frac{B_2}{\omega B_{2\alpha}}}{-\frac{A}{V_o} 1/2}\right)^4 (G_{1D}^2) - G_{1D}^2 = \omega^2(C_1+C_2)^2 - \left(\frac{\ln \frac{B_2}{\omega B_{2\alpha}}}{-\frac{A}{V_o} 1/2}\right)^4 \omega^2 C_1{}^2$$

and the following values are substituted:

$B_2 = 0.1$ lumen/m^2

$\omega B_{2\alpha} = 1.3 \times 10^4$ lumen/m^2/cycle

$C_1 = 9.8 \times 10^{-10}$ farad

$C_2 = 3.64 \times 10^{-9}$ farad

$\omega = (2\pi)$ (6000 cps)

$\frac{1}{V_o} 1/2 = 0.059$

Solving for G_{1D} gives:

$G_{1D} = 2.9 \times 10^{-5}/\Omega$.

DISTRIBUTION

	Copies
Chief, Bureau of Naval Weapons, Washington, D. C.	
RUME-3E	1
RMMP-43	1
SP-271 and SP 274	2
RRMA-221	1
FQ-1	1
RRMA-24	1
Chief, Bureau of Ships, Washington, D. C.	
Code 634B	1
Code 1500	1
Code 343	1
Library	1
Office of Naval Research, Washington D. C.	
Library	2
Director, Naval Research Laboratory, Washington, D. C.	
Code 2027	1
Code 6254, 5368 and 6210	3
Commanding Officer, U. S. Naval Propellant Plant, Indian Head, Maryland	
Library	2
J.E. Wilson and H. B. Alexander	2
Director, U. S. Naval Engineering Experiment Station, Annapolis, Maryland	
Code 760	1
Code 762	1
Commanding General, Air Research Development Command, WADD, Wright-Patterson Air Force Base, Ohio	
WCRTLSA	1
WCRTR4	1
WCRTL4	1
Library	1
Commanding Officer, Springfield Armory, Springfield, Massachusetts	
Research and Development Branch	1
Library	1
Office, Chief of Ordnance, Washington, D. C.	
Library	1

DISTRIBUTION (Continued)

	Copies
Commanding Officer, Army Chemical Center, Maryland	
Library	1
P. Edmiston, Quality Assurance	1
T. M. Vining, Stat. Engr. Office	1
Headquarters, Army Chemical Center and Chemical Corps Materiel Command, Baltimore 1, Maryland	
Directorate of Industrial Operations	1
Munitions Section	1
Commanding Officer, Fort Belvoir, Virginia	
Engineering Research and Development Lab	1
Commander, U. S. Naval Ordnance Test Station, China Lake, California	
Code 5510	1
Code 4537	1
Code 45335	1
Commanding General, Ordnance Ammunition Center, Joliet, Illinois	
Library	1
Inspection Division	1
Commanding General, Detroit Arsenal, Center Line Michigan	
Library	2
S. Sobak	1
Commanding Officer, Redstone Arsenal, Huntsville, Ala.	
Technical Library	2
Commanding Officer, Watertown Arsenal, Watertown 72, Massachusetts	
Chief, Technical Information Section	1
OMRO (Mr. Darcy)	1
Commanding Officer, Aberdeen Proving Ground, Maryland	
Technical Library	1
Physical Test Laboratory	1
Commanding Officer, Watervliet Arsenal, Watervliet,N.Y.	
C. A. Penrose, R&E Division	1

DISTRIBUTION (Continued)

	Copies
Commander, Boston Naval Shipyard, Massachusetts	
Code 375	1
Code 370	1
Commander, Philadelphia Naval Shipyard, Philadelphia 12, Pennsylvania	
Code 249c	1
Commanding Officer, Frankford Arsenal, Philadelphia 27, Pennsylvania	
ORDBA-MIS	1
Pitman-Dunn Laboratories (Mr. Roffman & Mr. LeVino)	2
Technical Library	1
Commanding Officer, Naval Air Engineering Facility, Naval Air Materiel Center, Philadelphia 12, Penna.	
F. S. Williams	1
Library	1
Commanding Officer, U. S. Naval Shipyard, Brooklyn 1, New York	
Code 982	1
Boston Air Procurement District, Boston Army Base, Boston 10, Massachusetts	
J. T. Hannon, Ch., Quality Control	1
Commanding Officer, Philadelphia Quartermaster Depot, Philadelphia 45, Pennsylvania	
Technical Library	1
Commanding Officer, Picatinny Arsenal, Dover, N. J.	
ORDBB-NI-3	1
Technical Library	2
ORDBB Mr. Silvestro	1
J. Hasko	1
Commander, Norfolk Naval Shipyard, Portsmouth, Virginia	
Code 304 H. H. Walkup	1
Commanding Officer, U. S. Naval Proving Ground, Dahlgren, Virginia	
Technical Library	1
Commander, Portsmouth Naval Shipyard, Portsmouth, New Hampshire	
Code 375	1
Code 251	1
Technical Library	1

DISTRIBUTION (Continued)

	Copies
Commanding Officer, U. S. Naval Ammunition Depot, Concord, California	
F. Hund, Quality Evaluation Laboratory	1
P. M. Seaman	1
J. Cusick	1
Library	1
Commander, U. S. Naval Ordnance Laboratory, Corona, California	
Code 5531	1
Code 65	1
Library	1
Commanding Officer, Tinker Air Force Base, Oklahoma	
OCAMA, Lt. Mayer	1
Commanding Officer, Naval Air Station, Corpus Christi, Texas	1
U. S. Naval Ammunition Depot, General Services Department, Crane, Indiana	
Attn: Depot Library	2
Commanding Officer, U. S. Naval Weapons Station, Yorktown, Virginia	
R&D Division, B. Carr, Jr.	1
R&D Division, R. Smoot	1
Library	1
Mare Island Naval Shipyard, Vallejo, California	
Code 303	1
Code 370	1
Commanding Officer, U. S. Naval Electronics Laboratory, San Diego, Californis	
Library	1
U. S. Radium Corporation, Whippany, New Jersey	
Dr. Wm. H. Byler Contract NOrd 18369	2
Army Research Office, Arlington Hall Station, Virginia	
Lt. Col. L. G. Klinker	1
Commanding Officer, Naval Air Station, Jacksonville Florida	
Library	1

SPECIAL DISTRIBUTION LIST

Members of POLARIS/MINUTEMAN/PERSHING Nondestructive Test Committee as listed below:

	Copies
AOMC, Redstone Arsenal, Huntsville, Alabama	
ORDAB-RPS Mr. T.N.L. Pughe)	1
Allegany Ballistics Laboratory, P. O. Box 210, Cumberland, Maryland	
E. D. Harvey	1
R. Downey	1
Aerojet General Corporation, Sacramento, California	
Dept 6600	1
5270	1
3770	1
Aerojet General Nucleonics, San Ramon, California	
Mr. P. Underhill	1
Ballistic Systems Division, Air Force Unit Post Office, Los Angeles 45, California	
Major Harned	1
Dr. P. K. Leatherman	1
Boeing Company, Seattle, Washington	
J. M. Baker	1
BuWepsRep, Sunnyvale, California	
SPL-40	1
BuWepsRep, Sacramento, California	
SPLA-44	1
BuWepsRep, Bacchus, Utah	
SPLB 40	1
BuWepsRep, ABL, P. O. Box 210, Cumberland, Md.	
R. J. Mascis	1
Commander, Hill Air Force Base, Utah	
Alex Peresich	1
Hercules Powder Company, Bacchus Works, Magna, Utah	
J. R. McWhirter	1
Sanford Gross	1
Jet Propulsion Laboratory, Pasadena, California	
G. W. Lewis	1

DISTRIBUTION (Continued)

	Copies
Lockheed Missile and Space Company, Sunnyvale, California	
LMSC 81-34	1
81-51	1
The Martin/Marietta Company, Orlando Division, Orlando, Florida	
MP-14 M. G. Miller	1
MP-348	1
LACREP, Aerojet General Corporation, California	2
Naval Research Development Laboratory, San Francisco, California	
Code 942	1
Solid Propellant Information Agency, Johns Hopkins, Applied Physics Laboratory, Silver Spring, Maryland	1
Space Technology Laboratory, No. One Space Park, Redondo Beach, California	
Harry Taylor	1
Thiokol Chemical Corporation, Brigham City, Utah	
M. Rubin	1
D. W. Rathmann	1
Thiokol Chemical Corporation, Wasatch Division, Tremonton, Utah	
E. C. Goforth	1
D. Liddell	1
Thiokol Chemical Corporation, Redstone Division, Huntsville, Alabama	
W. W. Mills	1
Thiokol Chemical Corporation, Longhorn Division, Marshall, Texas	
H. T. Bowman	1
Los Alamos Scientific Laboratory, New Mexico	
Dr. G. H. Tenney	1

CATALOGING INFORMATION FOR LIBRARY USE

BIBLIOGRAPHIC INFORMATION

Descriptors	Codes	Descriptors	Codes
Source NOL technical report	NOLTR	Security Classification and Code Count Unclassified - 23	U023
Report Number 61-115	610115	Circulation Limitation	
Report Date 15 April 1962	0462	Circulation Limitation or Bibliographic	
		Bibliographic (Suppl., Vol., etc.)	

SUBJECT ANALYSIS OF REPORT

Descriptors	Codes	Descriptors	Codes	Descriptors	Codes
Solid-state	SOLS	Fluorescent	FLRS		
Intensifying	ITEN	Low	LOWE		
Screens (Operation)	SCREI	Energies	ENER		
Screens (Characteristics)	SCREC	Sodium	SODI		
Screens (Evaluation)	SCREV	Iodide	IODI		
Screens	SCRE	Crystal	CRYS		
U.S. Radium Corp.	USRD	High	HIGH		
Image	IMAG	Equation	EQUA		
Brightness	BRIG	Parameters	PARA		
Measurement	MEAU	Industrial	INDS		
X-ray	XRAY	Radiography	RADG		
Comparison	CMRI				

Naval Ordnance Laboratory, White Oak, Md.
(NOL technical report 61-115)
AN INVESTIGATION OF THE OPERATING CHARACTERISTICS OF THE SOLID STATE INTENSIFYING SCREENS, by J.A. Holloway. 15 April 1962. v.p. charts, diagrs. Tasks RUME 3E 006/212 1/F008-10 004 and RMMP 33 063. UNCLASSIFIED

Experimental data is presented on the characteristics of solid state intensifying screens manufactured by U.S. Radium Corporation. Brightness measurements as a function of x-ray intensity from 90 kvp to 10 Mev are given. Comparison of screen characteristics is made relative to standard fluorescent screen at low x-ray energies and to NaI crystal at high energies. Increased brightness and contract of solid state screen is demonstrated. Equation describing screen brightness in terms of various screen parameters is derived.

1. Screens, Intensifying
2. Sodium iodide
3. Screens - Brightness
4. Screens, Fluorescent
5. X-rays - Intensity
6. Radiography, Industrial

I. Title
II. Holloway, James A.
III. Project
IV. Project

Naval Ordnance Laboratory, White Oak, Md.
(NOL technical report 61-115)
AN INVESTIGATION OF THE OPERATING CHARACTERISTICS OF THE SOLID STATE INTENSIFYING SCREENS, by J.A. Holloway. 15 April 1962. v.p. charts, diagrs. Tasks RUME 3E 006/212 1/F008-10 004 and RMMP 33 063. UNCLASSIFIED

Experimental data is presented on the characteristics of solid state intensifying screens manufactured by U.S. Radium Corporation. Brightness measurements as a function of x-ray intensity from 90 kvp to 10 Mev are given. Comparison of screen characteristics is made relative to standard fluorescent screen at low x-ray energies and to NaI crystal at high energies. Increased brightness and contract of solid state screen is demonstrated. Equation describing screen brightness in terms of various screen parameters is derived.

1. Screens, Intensifying
2. Sodium iodide
3. Screens - Brightness
4. Screens, Fluorescent
5. X-rays - Intensity
6. Radiography, Industrial

I. Title
II. Holloway, James A.
III. Project
IV. Project

Naval Ordnance Laboratory, White Oak, Md.
(NOL technical report 61-115)
AN INVESTIGATION OF THE OPERATING CHARACTERISTICS OF THE SOLID STATE INTENSIFYING SCREENS, by J.A. Holloway. 15 April 1962. v.p. charts, diagrs. Tasks RUME 3E 006/212 1/F008-10 004 and RMMP 33 063. UNCLASSIFIED

Experimental data is presented on the characteristics of solid state intensifying screens manufactured by U.S. Radium Corporation. Brightness measurements as a function of x-ray intensity from 90 kvp to 10 Mev are given. Comparison of screen characteristics is made relative to standard fluorescent screen at low x-ray energies and to NaI crystal at high energies. Increased brightness and contract of solid state screen is demonstrated. Equation describing screen brightness in terms of various screen parameters is derived.

1. Screens, Intensifying
2. Sodium iodide
3. Screens - Brightness
4. Screens, Fluorescent
5. X-rays - Intensity
6. Radiography, Industrial

I. Title
II. Holloway, James A.
III. Project
IV. Project

Naval Ordnance Laboratory, White Oak, Md.
(NOL technical report 61-115)
AN INVESTIGATION OF THE OPERATING CHARACTERISTICS OF THE SOLID STATE INTENSIFYING SCREENS, by J.A. Holloway. 15 April 1962. v.p. charts, diagrs. Tasks RUME 3E 006/212 1/F008-10 004 and RMMP 33 063. UNCLASSIFIED

Experimental data is presented on the characteristics of solid state intensifying screens manufactured by U.S. Radium Corporation. Brightness measurements as a function of x-ray intensity from 90 kvp to 10 Mev are given. Comparison of screen characteristics is made relative to standard fluorescent screen at low x-ray energies and to NaI crystal at high energies. Increased brightness and contract of solid state screen is demonstrated. Equation describing screen brightness in terms of various screen parameters is derived.

1. Screens, Intensifying
2. Sodium iodide
3. Screens - Brightness
4. Screens, Fluorescent
5. X-rays - Intensity
6. Radiography, Industrial

I. Title
II. Holloway, James A.
III. Project
IV. Project

Naval Ordnance Laboratory, White Oak, Md.
(NOL technical report 61-115)
AN INVESTIGATION OF THE OPERATING CHARACTERISTICS OF THE SOLID STATE INTENSIFYING SCREENS, by J.A. Holloway. 15 April 1962. v.p. charts, diagrs. Tasks RUME 3E 006/212 1/F008-10 004 and RMMP 33 063. UNCLASSIFIED

Experimental data is presented on the characteristics of solid state intensifying screens manufactured by U.S. Radium Corporation. Brightness measurements as a function of x-ray intensity from 90 kvp to 10 Mev are given. Comparison of screen characteristics is made relative to standard fluorescent screen at low x-ray energies and to NaI crystal at high energies. Increased brightness and contract of solid state screen is demonstrated. Equation describing screen brightness in terms of various screen parameters is derived.

1. Screens, Intensifying
2. Sodium iodide
3. Screens - Brightness
4. Screens, Fluorescent
5. X-rays - Intensity
6. Radiography, Industrial

I. Title
II. Holloway, James A.
III. Project
IV. Project

Naval Ordnance Laboratory, White Oak, Md.
(NOL technical report 61-115)
AN INVESTIGATION OF THE OPERATING CHARACTERISTICS OF THE SOLID STATE INTENSIFYING SCREENS, by J.A. Holloway. 15 April 1962. v.p. charts, diagrs. Tasks RUME 3E 006/212 1/F008-10 004 and RMMP 33 063. UNCLASSIFIED

Experimental data is presented on the characteristics of solid state intensifying screens manufactured by U.S. Radium Corporation. Brightness measurements as a function of x-ray intensity from 90 kvp to 10 Mev are given. Comparison of screen characteristics is made relative to standard fluorescent screen at low x-ray energies and to NaI crystal at high energies. Increased brightness and contract of solid state screen is demonstrated. Equation describing screen brightness in terms of various screen parameters is derived.

1. Screens, Intensifying
2. Sodium iodide
3. Screens - Brightness
4. Screens, Fluorescent
5. X-rays - Intensity
6. Radiography, Industrial

I. Title
II. Holloway, James A.
III. Project
IV. Project

Naval Ordnance Laboratory, White Oak, Md.
(NOL technical report 61-115)
AN INVESTIGATION OF THE OPERATING CHARACTERISTICS OF THE SOLID STATE INTENSIFYING SCREENS, by J.A. Holloway. 15 April 1962. v.p. charts, diagrs. Tasks RUME 3E 006/212 1/F008-10 004 and RMMP 33 063. UNCLASSIFIED

Experimental data is presented on the characteristics of solid state intensifying screens manufactured by U.S. Radium Corporation. Brightness measurements as a function of x-ray intensity from 90 kvp to 10 Mev are given. Comparison of screen characteristics is made relative to standard fluorescent screen at low x-ray energies and to NaI crystal at high energies. Increased brightness and contract of solid state screen is demonstrated. Equation describing screen brightness in terms of various screen parameters is derived.

1. Screens, Intensifying
2. Sodium iodide
3. Screens - Brightness
4. Screens, Fluorescent
5. X-rays - Intensity
6. Radiography, Industrial

I. Title
II. Holloway, James A.
III. Project
IV. Project

Naval Ordnance Laboratory, White Oak, Md.
(NOL technical report 61-115)
AN INVESTIGATION OF THE OPERATING CHARACTERISTICS OF THE SOLID STATE INTENSIFYING SCREENS, by J.A. Holloway. 15 April 1962. v.p. charts, diagrs. Tasks RUME 3E 006/212 1/F008-10 004 and RMMP 33 063. UNCLASSIFIED

Experimental data is presented on the characteristics of solid state intensifying screens manufactured by U.S. Radium Corporation. Brightness measurements as a function of x-ray intensity from 90 kvp to 10 Mev are given. Comparison of screen characteristics is made relative to standard fluorescent screen at low x-ray energies and to NaI crystal at high energies. Increased brightness and contract of solid state screen is demonstrated. Equation describing screen brightness in terms of various screen parameters is derived.

1. Screens, Intensifying
2. Sodium iodide
3. Screens - Brightness
4. Screens, Fluorescent
5. X-rays - Intensity
6. Radiography, Industrial

I. Title
II. Holloway, James A.
III. Project
IV. Project

UNCLASSIFIED